

Universal quantum algorithmic cooling on a quantum computer

Pei Zeng,^{1,*} Jinzhao Sun,^{2,3,†} and Xiao Yuan^{2,‡}

¹*Pritzker School of Molecular Engineering, The University of Chicago, Illinois 60637, USA*

²*Center on Frontiers of Computing Studies, Peking University, Beijing 100871, China*

³*Clarendon Laboratory, University of Oxford, Oxford OX1 3PU, UK*

(Dated: October 1, 2021)

Quantum cooling, a deterministic process that drives any state to the lowest eigenstate, has been widely used from studying ground state properties of chemistry and condensed matter quantum physics, to general optimization problems. However, the cooling procedure is generally non-unitary, hence its realization on a quantum computer either requires deep circuits or assumes specific input states with variational circuits. Here, we propose universal quantum cooling algorithms that overcome these limitations. By utilizing a dual phase representation of decaying functions, we show how to universally and deterministically realize a general cooling procedure with shallow quantum circuits. We demonstrate its applications in cooling an arbitrary input state with known ground state energy, corresponding to satisfactory, linear algebra tasks, and quantum state compiling tasks, and preparing unknown eigenvalues and eigenstates, corresponding to quantum many-body problems. Compared to quantum phase estimation, our method uses only one ancillary qubit and much shallower circuits, showing exponential improvement of the circuit complexity with respect to the final state infidelity. We numerically benchmark the algorithms for the 8-qubit Heisenberg model and verify its feasibility for accurately finding eigenenergies and obtaining eigenstate measurements. Our work paves the way for efficient and universal quantum algorithmic cooling with near-term as well as universal fault-tolerant quantum devices.

Introduction.— A large class of tasks, whether finding ground states [1, 2], studying low temperature physics [3, 4], solving optimization problems [5, 6], or even simulating quantum dynamics [7], can be abstracted as a cooling problem. Among the various task specific classical algorithms — such as perturbation theories [8–10], variational approaches [11, 12], self-consistent embedding methods [13, 14], machine learning [15–17], etc — imaginary time evolution [18] defines a natural and universal cooling procedure. Consider a Hamiltonian H , the imaginary time evolution $e^{-\tau H}$ with a real-valued time τ monotonically lower down the average energy and deterministically drives an arbitrary pure state to the lowest eigenstate that has a nonzero overlap. Despite being mathematically universal, realizing imaginary time evolution for an arbitrary Hamiltonian is by no means an easy problem. The notorious sign problem [19, 20] in Monte Carlo implementation of imaginary time evolution has limited its usage for solving general strongly correlated problems [21, 22].

Can we realize a cooling procedure more efficiently on a quantum computer? The answer is yes! The most prominent algorithm is quantum phase estimation [23, 24], which efficiently projects an arbitrary input quantum state to an eigenstate of the Hamiltonian, given the input state has a nonvanishing overlap with the target eigenstate. However, quantum phase estimation generally requires a deep circuit that is only realizable with a universal quantum computer [25, 26]. With near-term

noisy intermediate-scale quantum devices, variational approaches has been developed to emulate the imaginary time evolution with fixed or adaptive parametrized quantum circuits [27–31]. Nevertheless, whether such circuits exist or how to efficiently find them still remains unclear [32–35]. Furthermore, whether there exists more efficient cooling procedures and how to efficiently realize them is an open problem.

Here, we propose a new paradigm for simulating general quantum cooling procedures on a quantum computer. For a general decaying function $g(h)$, such as $g = e^{-|h|}$ or $g = e^{-h^2}$, we show how to realize a general cooling procedure $g(\tau H)$ for Hamiltonian H using solely real time evolution and proper classical post-processing. The algorithm essentially implements a general non-Hermitian dynamics, and it can efficiently find energy spectra and corresponding eigenstates, for any initial states that have nonvanishing overlaps with the target state. Compared to quantum phase estimation, our method only needs a much shallower circuit with only one ancillary qubit. Compared to variational approaches, our algorithm works deterministically without any assumption on parametrized circuits.

In the following, we first propose the framework for quantum algorithmic cooling with general decaying functions, which suffices to define a quantum cooling procedure as long as its dual phase representation via Fourier transformation has bounded norms and good approximations with finite frequencies. Then we discuss its application for Hamiltonians with known and unknown eigenenergies. We analyze the resource cost — circuit depth and sampling cost — for the algorithm and numerically test it for the 8-qubit Heisenberg model. The results verify the feasibility of quantum algorithmic

* peizeng.phy@gmail.com

† jinzhao.sun@physics.ox.ac.uk

‡ xiaoyuan@pku.edu.cn

cooling with near-term and universal fault-tolerant quantum computers.

Quantum algorithmic cooling.— We start with a real-valued function $g(h)$ satisfying strictly non-increasing absolute value, $|g(h')| < |g(h)|$, $\forall h' > h > 0$ or $h' < h < 0$ [36], and vanishing asymptotic value, $\lim_{\tau \rightarrow \infty} |g(\tau h')/g(\tau h)| = 0$, $\forall h' > h > 0$ or $h' < h < 0$ [36], and $\lim_{\tau \rightarrow \infty} |g(\tau h)/g(0)| = 0$, $\forall |h| > 0$. Consider a positive Hamiltonian $H = \sum_i E_i |u_i\rangle \langle u_i|$ with eigenstates $\{|u_i\rangle\}$ and eigenvalues $E_i \geq 0$ [37], it defines a cooling procedure $g(\tau H)$ with Hamiltonian H and real-valued time τ for an arbitrary input state $|\psi_0\rangle = \sum_i c_i |u_i\rangle$ as

$$|\psi(\tau)\rangle = \frac{g(\tau H) |\psi_0\rangle}{\|g(\tau H) |\psi_0\rangle\|} = \frac{\sum_i g(\tau E_i) c_i |u_i\rangle}{\sum_i p_i g(\tau E_i)^2}, \quad (1)$$

with $p_i = |c_i|^2$. Since for larger eigenvalues the function $g(\tau E_i)$ decreases faster with τ , the amplitudes of the normalized state $|\psi(\tau)\rangle$ concentrate to lower eigenstates, and the evolved state asymptotically approximates the lowest eigenstate $|u_i\rangle$ with nonzero c_i for sufficiently large τ . A notable example is the exponential decreasing function $g(h) = e^{-|h|}$, corresponding to imaginary time evolution $g(\tau H) = e^{-\tau H}$ for positive H .

Since a cooling evolution $g(\tau H)$ is not a unitary, its realization on a quantum computer is not straightforward. For imaginary time evolution, a conventional strategy assumes a special input state, such as an eigenstate or the infinite temperature thermal state, and realize the evolution via Monte Carlo sampling [3] or adiabatic state preparation with phase estimation [4]. Such methods generally require a deep quantum circuit with many ancillary qubits. Another way uses variational methods with shallow parametrized circuits [27, 29–31, 38], which however relies on the strong expressivity power of the circuits [32–35]. Meanwhile, both methods are limited to specific input states.

Here, we propose a universal approach for realizing a general cooling function without the above limitations. We first consider the dual form of $g(h)$ via its Fourier transform $g(h) = \frac{1}{2\pi} \int_{-\infty}^{\infty} f(x) e^{ixh} dx$, with the inverse transform $f(x) = \int_{-\infty}^{\infty} g(h) e^{-ixh} dh$. Given the norm of $f(x)$ defined as $\|f\| = \int_{-\infty}^{\infty} |f(x)| dx$, we consider the normalized function $p(x) = |f(x)|/\|f\|$ and we have

$$g(h) = c \int_{-\infty}^{\infty} e^{i\theta_x} p(x) e^{ixh} dx, \quad (2)$$

where $c = \|f\|/2\pi$ and $e^{i\theta_x} = f(x)/|f(x)|$. The function $g(h)$ is *realizable* if the following conditions hold.

C1: The normalization $\|f\|$ or c is finite.

C2: $|1 - \int_{-L(\varepsilon)}^{L(\varepsilon)} p(x) dx| \leq \varepsilon$, $\forall \varepsilon \geq 0$, $\exists L(\varepsilon) = \mathcal{O}(\text{poly}(\frac{1}{\varepsilon}))$.

The first condition implies a finite norm of $\|f\|$ and the second condition implies that a finite frequency in $[-L(\varepsilon), L(\varepsilon)]$ with $L(\varepsilon) = \mathcal{O}(\text{poly}(1/\varepsilon))$ is sufficient

TABLE I. Representative cooling functions $g(h)$. Here $f(x)$ corresponds to Fourier transform of $g(h)$, *C1* refers to $c = \|f\|/2\pi$ which should be finite, *C2* refers to $L(\varepsilon)$ which should be less than $\mathcal{O}(\text{poly}(\frac{1}{\varepsilon}))$, $\eta(\text{true/false}) = 1/0$, $\text{sinc}(x) = \frac{\sin(x)}{x}$, $\text{sech}(x) = \frac{2}{e^x + e^{-x}}$. Except for the rectangular function, the other four functions satisfy *C1* and *C2*.

Type	$g(h)$	$f(x)$	<i>C1</i>	<i>C2</i>
Rectangular	$\eta(h \leq 1/2)$	$\text{sinc}(x/2\pi)$	∞	∞
Triangle	$(1 - h)\eta(h \leq 1)$	$\text{sinc}^2(x/2\pi)$	2π	$6/\varepsilon$
Exponential	$e^{- h }$	$\frac{2}{x^2 + 1}$	1	$2/(\pi\varepsilon)$
Gaussian	e^{-h^2}	$\sqrt{\pi} e^{-x^2/4}$	1	$2\sqrt{\ln(1/\varepsilon)}$
Hyperbolic	$\text{sech}(h)$	$\pi \text{sech}(\pi x/2)$	1	$\frac{2}{\pi} \ln(1/\varepsilon)$

for approximating the normalized function $g(h)/c$, i.e., $|g(h)/c - \int_{-L(\varepsilon)}^{L(\varepsilon)} p(x) e^{ixh + \theta_x} dx| \leq \varepsilon$. In Table I, we give several examples of $g(h)$. Since our examples have zero phase, for a simpler presentation, we set the phase terms to be 0 in the following discussion. Although, our following discussion naturally generalizes to the case with nonzero phases. The detailed analysis of the cooling functions is in Appendix A.

With the normalized dual phase representation $p(x)$ of $g(h)$, the cooling procedure of Eq. (1) becomes

$$|\psi(\tau)\rangle \propto \int_{-\infty}^{\infty} dp(x) |\phi(x\tau)\rangle, \quad (3)$$

which is now a superposition of real time evolved states $|\phi(x\tau)\rangle = e^{ix\tau H} |\psi_0\rangle$ with amplitudes $dp(x) = p(x)dx$. The linear combination of unitary algorithm [39–41] could be exploited to create the superposition with a quantum circuit $e^{ix\tau H}$ and x conditioned on a continuous variable ancillary state $\int_{-\infty}^{\infty} dp(x) |x\rangle$. However, creating such continuous variable states is challenging with a digital quantum computer. Here we propose an experimentally more feasible and efficient way to effectively realize the superposition.

Instead of preparing the whole quantum state of Eq. (3), we change the goal to obtain arbitrary observable expectation values. Specifically, we aim to measure an observable O of the evolved state $|\psi(\tau)\rangle$, i.e.,

$$\langle O \rangle_{\psi(\tau)} = \langle \psi(\tau) | O | \psi(\tau) \rangle = \frac{N_{\tau}(\psi_0, O)}{D_{\tau}(\psi_0)}, \quad (4)$$

where $N_{\tau}(\psi_0, O) = \int_{-\infty}^{\infty} \int_{-\infty}^{\infty} dp(x, x') \langle \phi(x'\tau) | O | \phi(x\tau) \rangle$ and $D_{\tau}(\psi_0) = \int_{-\infty}^{\infty} \int_{-\infty}^{\infty} dp(x, x') \langle \phi(x'\tau) | \phi(x\tau) \rangle$ with $dp(x, x') = p(x)p(x')dx dx'$. Here $D_{\tau}(\psi_0)$ can be simplified as $D_{\tau}(\psi_0) = \int_{-\infty}^{\infty} d\tilde{p}(y) \langle \psi_0 | e^{iy\tau H} | \psi_0 \rangle$ with $d\tilde{p}(y) = \tilde{p}(y)dy$ and $\tilde{p}(y) = \frac{1}{2} \int_{-\infty}^{\infty} p(\frac{z+y}{2})p(\frac{z-y}{2})dz$. For the numerator $N_{\tau}(\psi_0, O)$, we can efficiently obtain it by sampling the distribution $dp(x, x')$ and then estimating the mean value $\mathbb{E}_{x, x'} \langle \phi(x'\tau) | O | \phi(x\tau) \rangle$, where each term is realizable on a quantum computer with the Hadamard

test circuit. We can similarly obtain the denominator $D_\tau(\psi_0)$ by estimating $\mathbb{E}_y \langle \psi_0 | e^{iy\tau H} | \psi_0 \rangle$ with probability $d\tilde{p}(y)$. Therefore, we only need a quantum computer to efficiently implement state overlaps like $\langle \psi_0 | U | \psi_0 \rangle$ with U being either $e^{-ix'\tau H} O e^{ix\tau H}$ or $e^{iy\tau H}$, and then we can effectively obtain the time-dependent expectation value of any observable by post-processing the measurement outcomes.

Now, the only potential issue is the integration with an infinite frequency, leading to infinite real time evolution. Fortunately, sacrificing a small error ε , we can consider a cutoff of the integral from $[-\infty, \infty]$ to $[-L(\varepsilon), L(\varepsilon)]$ to avoid the problem. Denote the numerator and denominator with cutoffs to be $\tilde{N}_\tau(\psi_0, O)$ and $\tilde{D}_\tau(\psi_0)$, we have $|\tilde{N}_\tau(\psi_0, O) - N_\tau(\psi_0, O)| \leq (2\varepsilon + \varepsilon^2) \|O\|_\infty$ and $|\tilde{D}_\tau(\psi_0) - D_\tau(\psi_0)| \leq \varepsilon$. Note that the truncation $L(\varepsilon)$ is linear or logarithmic to $1/\varepsilon$ for the valid cooling functions in Table I. Therefore, the maximal evolution time for obtaining $\langle O \rangle_{\psi(\tau)}$ within error $\varepsilon > 0$ scales as $\mathcal{O}(\tau \|O\|_\infty / \varepsilon)$, $\mathcal{O}(\tau \ln(\|O\|_\infty / \varepsilon))$, or even $\mathcal{O}(\tau \sqrt{\ln(\|O\|_\infty / \varepsilon)})$, which is linear and at best square root logarithmic to $1/\varepsilon$. At last, we can randomly sample a frequency in $[-L(\varepsilon), L(\varepsilon)]$ and approximate $N_\tau(\psi_0, O)$ and $D_\tau(\psi_0, O)$ with small sampling errors. We show shortly the sample complexity and its dependence on the energy gap, the initial state overlap, and the final state fidelity.

Applications.— For short time τ , the cooling procedure could be applied for simulating general non-hermitian dynamics by Trotterizing the real and imaginary evolution. On the other hand, cooling with sufficient large τ would deterministically drive any state to an eigenstate. Here we focus on the latter part and consider applications of quantum algorithmic cooling for quantum systems with known and unknown eigenvalues. The detailed algorithms can be found in Appendix B.

First, we apply it to cool down states for Hamiltonians H with a known ground state energy $E_0 \geq 0$, corresponding to satisfactory problems [5, 6, 42–44], linear algebra tasks [45–47], quantum state compiling [48–52], quantum error correction [53, 54], etc. For an initial state $|\psi_0\rangle = \sum_i c_i |u_i\rangle$ with a nonvanishing $p_0 = |c_0|^2$, our proposed algorithm can effectively cool down $|\psi_0\rangle$ and deterministically drive it to the ground state $|u_0\rangle$. Specifically, we can obtain the average of any observable as if we had obtained the evolved state. Nevertheless, we have to be more careful with Eq. (4) since the observable expectation value is obtained from the ratio between $N_\tau(\psi_0, O)$ and $D_\tau(\psi_0)$, where the latter originates from state normalization. Specifically, when $E_0 > 0$, the denominator

$$D_\tau(\psi_0) = \langle \psi_0 | g(\tau H)^2 | \psi_0 \rangle / c^2, \quad (5)$$

may decrease exponentially with τ , where $c = (2\pi/\|f\|)^2$ is a constant. For example, when $g(h) = e^{-|h|}$, we have $D_\tau(\psi_0) = \sum_i p_i e^{-2\tau E_i} < p_0 e^{-2\tau E_0}$ with $p_i = |c_i|^2$. In this case, the numerator also decreases exponentially

with τ and we need an exponential number of samples to achieve a desired accuracy of the observable [55]. A simple strategy to circumvent the exponential decay is to shift the Hamiltonian by $-E_0$, so that the shifted ground state energy is 0. In this case, for large τ , the denominator $D_\tau(\psi_0)$ scales as p_0 , and the sample complexity would be independent of τ . Furthermore, it is not hard to see that for the valid cooling functions considered in Table I, the algorithm works for any eigenstate $|u_i\rangle$ with known eigenenergy E_i , by shifting the Hamiltonian by $-E_i$. The algorithm is efficient as long as the probability p_i is not too small.

For the second task, we consider more general problems with unknown (inaccurate) eigenenergy, such as chemistry or condensed matter problems [56–60]. A conventional approach for solving those problems is to first apply adiabatic state preparation to obtain an approximate state $|\psi_0\rangle = \sum_i c_i |u_i\rangle$ and then use quantum phase estimation to randomly project it to an eigenstate $|u_i\rangle$ with eigenenergy E_i and probability $p_i = |c_i|^2$ [1, 2]. The algorithmic cooling procedure can be applied to effectively realize the eigenstate projection. Starting with a guess E of an eigenenergy (for instance, obtained from classical methods), we shift the Hamiltonian by $-E$ and estimate the denominator $D_{\tau, \psi_0}(E)$ as

$$D_{\tau, \psi_0}(E) = \langle \psi_0 | g((H - E)\tau)^2 | \psi_0 \rangle / c^2. \quad (6)$$

Note that $D_{\tau, \psi_0}(E)$ is locally maximized to p_i/c^2 when $E = E_i$ is an eigenvalue of H , otherwise it exponentially decays with τ . Then we can scan the denominator $D_{\tau, \psi_0}(E)$ with different trial energy E and find the eigenvalues of H via the peaks of $D_{\tau, \psi_0}(E)$. Furthermore, the denominator $D_{\tau, \psi_0}(E)$ is

$$D_{\tau, \psi_0}(E) = \int_{-\infty}^{\infty} d\tilde{p}(y) e^{-iy\tau E} \langle \psi_0 | e^{iy\tau H} | \psi_0 \rangle, \quad (7)$$

where $\langle \psi_0 | e^{iy\tau H} | \psi_0 \rangle$ is obtained from quantum computers, and the information of E and the distribution $d\tilde{p}(y)$ only appears as the coefficient. Therefore $D_{\tau, \psi_0}(E)$ with different E could be obtained from different classical post-processing of the same measurement outcome $\langle \psi_0 | e^{iy\tau H} | \psi_0 \rangle$, making the algorithm very efficient without any dependence on E . Due to the monotonic feature of g , there also exist super efficient classical algorithms, such as binary search algorithms, to find peaks of $D_{\tau, \psi_0}(E)$.

In the above discussion, we have assumed a ‘good’ initial state that has a nonvanishing overlap with the target state, an assumption usually adopted in quantum phase estimation. To prepare such states, we could just use a classical approximated solution [11, 12], such as the Hartree Fock state or a tensor network solution, or we can apply adiabatic state preparation to enhance the state overlap [1, 2, 61]. Besides, one can use shallow parametrized quantum circuits and apply variational optimization to search for an approximated solution [62–64]. Integrating these approximation algorithms with

our quantum algorithmic cooling, it provides an efficient way to study eigenstates and eigenvalues of many-body quantum systems.

Error and resource estimation.— When applying the cooling algorithm in practice, we have to take the error caused by finite circuit depth and finite sampling number into consideration. There are three dominant factors limiting the precision of our estimation: the finite imaginary time τ , the cutoff x_m of the probability sampling of $p(x)$ or $\tilde{p}(y)$, and the finite sampling number N_M during the experiment. We now check the effect of these factors separately. The detailed analysis can be found in Appendix C.

In the ideal case of $\tau \rightarrow \infty$, the unnormalized resulting state is $g(\tau(H - E_j))|\psi_0\rangle \propto |u_j\rangle$, thus completely filtering out other eigenstate components besides $|u_j\rangle$. In practice, when the value of τ is finite, other eigenstate components remain and the unnormalized state becomes

$$|\tilde{\psi}(\tau)\rangle := g(\tau(H - E_j))|\psi_0\rangle = c_j|u_j\rangle + \sum_{i \neq j} c_i g(\tau\Delta_{ij})|u_i\rangle,$$

where $\Delta_{ij} := |E_i - E_j|$ is the energy gap between the i -th and j -th eigenstates. In this case, the non-zero amplitude $c_i g(\tau\Delta_{ij})$ will affect the fidelity of the prepared state and hence introduce errors to the estimation of $\langle O \rangle_{u_j}$. We denote the finite- τ estimation to be $\langle O \rangle_{\psi(\tau)}$. In the case, when τ is large such that $g(\tau\Delta_{ij}) \ll \langle u_i | O | u_i \rangle$, we can mainly consider the zeroth and first order term related to $g(\tau\Delta_{ij})$. The estimation difference is then given by

$$|\langle O \rangle_{\psi(\tau)} - \langle O \rangle_{u_j}| \approx 2p_j^{-1}|c_j| \left| \langle O \rangle_{u_j} \sum_{i \in \mathcal{N}(j)} g(\tau\Delta_{ij})|c_i| \right|.$$

Denote the error introduced from finite τ by ε_τ , we can suppress it by choosing the imaginary time to be $\tau \sim g^{-1}(\varepsilon_\tau p_j / \|O\|_\infty) \Delta_{\min}^{-1}$, where $g^{-1}(p)$ is the inverse of the cooling function $g(h)$ and $\Delta_{\min} = \min \Delta_{ij}$. In Appendix A, we show that the valid cooling functions in Table I all satisfy $g^{-1}(p) = \mathcal{O}(\log(1/p))$. Therefore, we can choose τ to be $\mathcal{O}(\log(\|O\|_\infty / (p_j \varepsilon_\tau)) \Delta_{\min}^{-1})$, which is logarithmic to the inverse state overlap $1/p_j$ and inverse error $1/\varepsilon_\tau$, and linear to the inverse gap $1/\Delta_{\min}$.

Next, we consider the error introduced from the cutoff of the integral. Denote the integral cutoff by x_m , which introduces cutoff errors $\varepsilon_x^{(1)}$ and $\varepsilon_x^{(2)} \|O\|_\infty$ in the estimation of $D_\tau(\psi_0)$ and $N_\tau(\psi_0, O)$, respectively. We can simply use the tail probability distribution to bound these two error terms,

$$\varepsilon_x^{(1)} \leq 2L^{-1}(x_m/\sqrt{2}), \quad \varepsilon_x^{(2)} \leq 2L^{-1}(x_m),$$

where $L^{-1}(x_m)$ is the inverse function of $L(\varepsilon)$. As a result, the cutoff value $x_m \leq \sqrt{2}L(\varepsilon_x/2)$ (suppose $\varepsilon_x^{(1)} = \varepsilon_x^{(2)} =: \varepsilon_x$). In Table I, we have shown that for the triangle and exponential cooling functions, we have

$L(\varepsilon) = \mathcal{O}(\text{poly}(\frac{1}{\varepsilon}))$, and for the Gaussian and secant hyperbolic cooling functions, we can achieve even better results $\mathcal{O}(\sqrt{\log(\frac{1}{\varepsilon})})$ or $L(\varepsilon) = \mathcal{O}(\log(\frac{1}{\varepsilon}))$. That is, with a reasonable cutoff $x_m \sim L(\varepsilon_x)$, we can greatly suppress the cutoff errors $\varepsilon_x^{(1)}$ and $\varepsilon_x^{(2)}$.

At last, we consider the shot noise introduced from finite samples. In the experiment, we use the quantum circuit to estimate the values of $\langle \phi(x'\tau) | O | \phi(x\tau) \rangle$ and $\langle \psi_0 | e^{iy\tau H} | \psi_0 \rangle$. A common approach to estimate these values is the Hadamard test. In Appendix B, we create unbiased estimators for these values based on the Hadamard test. Using the Hoeffding bound, we show that the statistical errors in the estimation of $D_\tau(\psi_0)$ and $N_\tau(\psi_0, O)$ are bounded by $\varepsilon_n^{(1)}$ and $\varepsilon_n^{(2)} \|O\|_\infty$ when the sampling number $N_M = \mathcal{O}(\varepsilon_n^{-2})$ (suppose $\varepsilon_n^{(1)} = \varepsilon_n^{(2)} =: \varepsilon_n$). In Appendix C4, we show that the estimation errors $\varepsilon_{x,n}$ on the observable O caused by the finite truncation x_m and samples N_M is approximately

$$|\langle \hat{O} \rangle_{\psi(\tau)}^{x_m} - \langle O \rangle_{\psi(\tau)}| \approx p_j^{-1}(\varepsilon_n + \varepsilon_x)(\langle O \rangle + \|O\|_\infty)$$

Now denote the total error by ε , we can choose $\varepsilon_\tau \sim \varepsilon_{x,n} \sim \varepsilon$ and further $\varepsilon_n \sim \varepsilon_x \sim \varepsilon p_j(\langle O \rangle + \|O\|_\infty)^{-1}$. Note that the maximum real time evolution is given by $t_m = \tau x_m$. As a result, the time and sample complexity of the universal cooling algorithm is

$$t_m \sim \mathcal{O}(\Delta_{\min}^{-1} \log(\|O\|_\infty / (\varepsilon p_j))) L(\varepsilon p_j(\langle O \rangle + \|O\|_\infty)^{-1}), \\ N_M \sim \mathcal{O}(1/(\varepsilon p_j)^2)(\langle O \rangle + \|O\|_\infty)^2. \quad (8)$$

For the Gaussian cooling function, we have $L(\varepsilon) = \mathcal{O}(\sqrt{\log(\frac{1}{\varepsilon})})$. Therefore, if we set $\langle O \rangle = \|O\|_\infty^2 = \mathcal{O}(1)$, the time and sample complexity for the Gaussian cooling function is simplified as

$$t_m \sim \mathcal{O}(\Delta_{\min}^{-1} \log(1/(\varepsilon p_j)) \sqrt{\log(1/(\varepsilon p_j))}), \\ N_M \sim \mathcal{O}(1/(\varepsilon p_j)^2). \quad (9)$$

Here, the time or circuit complexity is logarithmic to $1/(p_j \varepsilon_\tau)$, which is exponentially better than quantum phase estimation or adiabatic state preparation.

Numerical test.— Here we show numerical implementation of the algorithmic cooling method for estimating the energy spectra of the anisotropic Heisenberg Hamiltonian, $H = J \sum_i (\sigma_i^x \sigma_{i+1}^x + \sigma_i^y \sigma_{i+1}^y + 2\sigma_i^z \sigma_{i+1}^z) + \sum_i \sigma_i^z$, where $J = 1$ is the exchange coupling, σ_i^α ($\alpha = x, y, z$) is the Pauli operator on the i th site, $h = 1$ is strength of a uniform magnetic field in the z direction, and we impose periodic boundary condition. We consider the initial state in the computation basis as $|01010101\rangle$, which is close to the ground state and has nonzero overlap with a relatively small number of low-energy eigenstates. We first show how to determine the energy spectra using the cooling method with Gaussian function

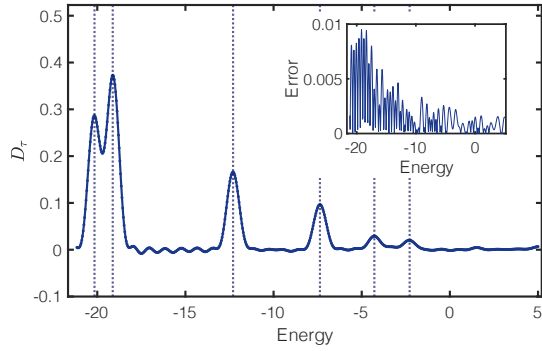


FIG. 1. Energy spectra search of the 8-site anisotropic Heisenberg model using the Gaussian cooling function. The solid line shows the denominator of D_τ with $\tau = 1.49$ and cutoff 4.55 calculated according to the precision in the main text. The dashed line shows the exact eigenenergy of the Heisenberg model. The figure inset shows the error of D_τ with respect to that under the exact cooling. We set $N_s = 10^5$ in the Monte Carlo sampling of the integral, and we use the expectation value for each sample that ignores measurement shot noise.

$g = \exp(-\tau^2(H - E_j)^2)$. Under the dual phase representation of the unphysical Gaussian function, the eigenenergy E_i maximizes the denominator $D_\tau(E)$ if the initial state has a nonvanishing spectral weight $|\langle \psi_0 | u_i \rangle|^2$ on the eigenstate $|u_i\rangle$. We can thus determine the eigenenergy by searching for the peaks of $D_\tau(E)$. Using a finite imaginary time $\tau = 1.49$ and cutoff $x_m = 4.55$ satisfying $\tau, x_m \propto \sqrt{2 \log(1/\epsilon)}$ for error ϵ with 10^5 number of samples for the integral, we show the energy spectra in Fig. 1. The maximum error introduced is below 0.01, which aligns with our error analysis.

Next, we show the error dependence of our algorithm in finding the eigenstate. We mainly focus on the time or circuit complexity, which is logarithmic to $1/\epsilon$ for the Gaussian cooling function. Suppose we aim to find the second eigenstate $|u_2\rangle$, which has the largest overlap with the initial state. Given the associated eigenenergy E_2 found by the above method, we now analyze the error introduced from finite imaginary time and cutoff. Here, we focus on the state infidelity of the normalized state after cooling and the target ideal eigenstate, which can be expressed as $\epsilon = 1 - \langle O \rangle_\tau$ with $O = |u_2\rangle \langle u_2|$. We show the error dependence on the imaginary time τ and the maximal total evolution time $t_m = \tau x_m$ with Gaussian and exponential cooling functions in Fig. 2(a1-a3) and (b1-b3), respectively. We plot the theoretical upper bound of the infidelity in the dashed line in the figures (assuming infinite samples) and realistic infidelity with a constant number of samples using dots. In Fig 2(a1) and (b1), we set the imaginary time τ according to the theoretical estimation, similarly in the spectra analysis, and fix the cutoff x_m , and we can see the exponential scaling with respect to the imaginary time τ . In Fig 2(a2) and (b2), we adjust both the imaginary time τ and the cutoff x_m , and again

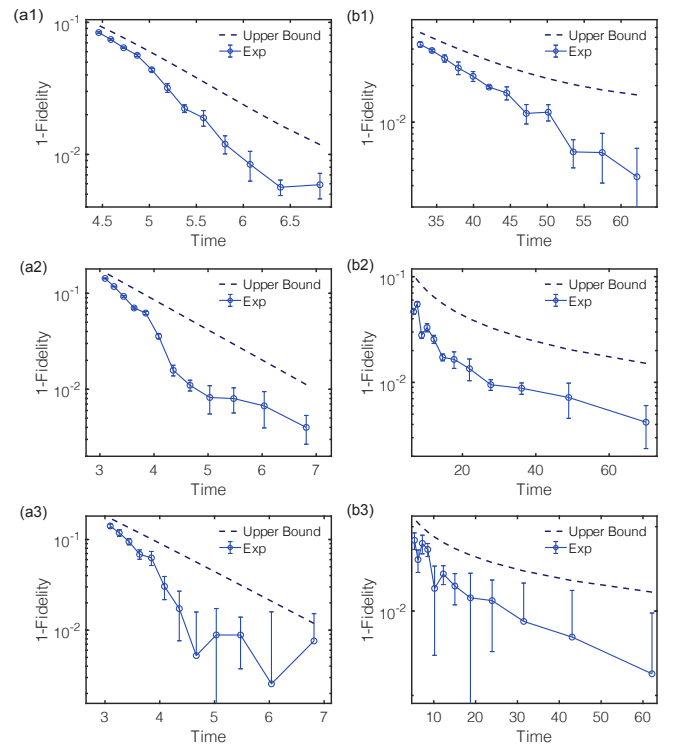


FIG. 2. Error dependence of the total evolution time with (a1-a3) Gaussian and (b1-b3) exponential cooling functions. In (a1) and (b1), we set the imaginary time τ according to the infidelity in the worst case, similarly in the spectrum analysis, and fix the cutoff x_m . In (a2) and (b2), we adjust both the imaginary time τ and the cutoff x_m , and study the infidelity versus maximal total time $t_m = \tau x_m$. We use 10^5 samples in the Monte Carlo sampling of the integral and ignore the measurement shot noise in (a1, a2, b1, b2). In (a3) and (b3), we further consider measurement shot noise, which introduces more instability of the infidelity. Nevertheless, we still observe the exponential and linear inverse decay of the infidelity for the Gaussian and exponential functions, respectively. The errorbar is the standard deviation of D_τ error over 10 independent repetitions of the entire setup. Dashed line: theoretical upper bound of the infidelity assuming infinite sample; Dots with error bar: realistic infidelity with a constant number of samples.

we see the exponential scaling with respect to the total evolution time t_m for the Gaussian cooling function, while it asymptotically becomes $1/\epsilon$ for the exponential cooling function. In Fig 2(a1, a2, b1, b2), we use 10^5 samples for calculating the integral, and ignore the shot noise of the quantum circuit measurement. In Fig 2(a3) and (b3), we further consider single-shot measurement outcomes and show the error dependence accordingly.

Conclusion & Discussion.— To summarize, we proposed an efficient way to implement general quantum cooling functions. By considering the dual form, we can effectively realize a non-unitary cooling procedure using real time evolution. We can apply the algorithm to prob-

lens with known and unknown eigenvalues and efficiently prepare the corresponding eigenstate as long as its overlap with the initial state is nonvanishing. Compared to quantum phase estimation, our algorithm uses a shallower circuit (exponentially smaller with respect to the inverse state infidelity and the state overlap) with fewer (only one) ancillary qubit. Compared to variational realization of imaginary time evolution, our method is deterministic. Therefore, our method is applicable to both near-term and fault-tolerant quantum computers when combined with variational quantum eigensolver or adiabatic state preparation.

We discuss two other potential applications of the universal cooling algorithm. One direction is to study system properties under the finite-temperature condition. Given the ability of implementing general cooling function or preparing eigenstates, one may combine other existing technique, such as Metropolis sampling [65], to effectively prepare thermal states and study finite-temperature physics. Another interesting application is to realize the evolution of a general Markovian quantum process, which is described by a non-Hermitian Hamiltonian [66]. In this case, we can decompose the Hamiltonian to the real and imaginary part, and further expand

the imaginary part using Fourier transform. In this way, we could simulate a general non-Hermitian dynamic process.

In this work, we mainly discuss the construction of cooling functions $g(h)$ based on the Fourier transform. We assumed that the cooling function $g(\tau h)$ becomes a single-peak δ function for sufficiently large τ . We remark that the Fourier transform is a universal tool to construct any non-unitary process else than cooling. As a simple example, one can create a “two-peak” cooling function to prepare a cat-like state, i.e., the superposition of two remote eigenstates. Meanwhile, we can explore different linear transforms of continuous or discrete functions, such as discrete Fourier transform and continuous wavelet transform, to study their possible usage in realizing even more general non-unitary processes.

Note added.—Recently, we became aware of a relevant work by Huo and Li [67], who considered a specific cooling function using the Fourier transform of the Lorentz-Gaussian function. They studied its application for realizing imaginary time evolution and discussed its combination with error mitigation for implementation with near-term quantum devices.

[1] D. S. Abrams and S. Lloyd, Quantum algorithm providing exponential speed increase for finding eigenvalues and eigenvectors, *Phys. Rev. Lett.* **83**, 5162 (1999).

[2] A. Aspuru-Guzik, A. D. Dutoi, P. J. Love, and M. Head-Gordon, Simulated quantum computation of molecular energies, *Science* **309**, 1704 (2005), <https://www.science.org/doi/pdf/10.1126/science.1113479>.

[3] K. Temme, T. J. Osborne, K. G. Vollbrecht, D. Poulin, and F. Verstraete, Quantum metropolis sampling, *Nature* **471**, 87 (2011).

[4] M.-H. Yung and A. Aspuru-Guzik, A quantum-quantum metropolis algorithm, *Proceedings of the National Academy of Sciences* **109**, 754 (2012), <https://www.pnas.org/content/109/3/754.full.pdf>.

[5] E. Farhi, J. Goldstone, and S. Gutmann, A quantum approximate optimization algorithm (2014), [arXiv:1411.4028 \[quant-ph\]](https://arxiv.org/abs/1411.4028).

[6] L. Zhou, S.-T. Wang, S. Choi, H. Pichler, and M. D. Lukin, Quantum approximate optimization algorithm: Performance, mechanism, and implementation on near-term devices, *Phys. Rev. X* **10**, 021067 (2020).

[7] I. Kassal, S. P. Jordan, P. J. Love, M. Mohseni, and A. Aspuru-Guzik, Polynomial-time quantum algorithm for the simulation of chemical dynamics, *Proceedings of the National Academy of Sciences* **105**, 18681 (2008), <https://www.pnas.org/content/105/48/18681.full.pdf>.

[8] A. A. Abrikosov, L. P. Gorkov, and I. E. Dzyaloshinski, *Methods of quantum field theory in statistical physics* (Courier Corporation, 2012).

[9] P.-O. Löwdin, Studies in perturbation theory. x. lower bounds to energy eigenvalues in perturbation-theory ground state, *Phys. Rev.* **139**, A357 (1965).

[10] J. Sun, S. Endo, H. Lin, P. Hayden, V. Vedral, and X. Yuan, Perturbative quantum simulation, arXiv preprint [arXiv:2106.05938](https://arxiv.org/abs/2106.05938) (2021).

[11] A. Szabo and N. S. Ostlund, *Modern Quantum Chemistry: Introduction to Advanced Electronic Structure Theory* (Courier Corporation, 2012).

[12] R. Orús, Tensor networks for complex quantum systems, *Nature Reviews Physics* **1**, 538 (2019).

[13] D. Sholl and J. A. Steckel, *Density Functional Theory: a Practical Introduction* (John Wiley & Sons, 2011).

[14] G. Knizia and G. K.-L. Chan, Density matrix embedding: A simple alternative to dynamical mean-field theory, *Phys. Rev. Lett.* **109**, 186404 (2012).

[15] G. Carleo and M. Troyer, Solving the quantum many-body problem with artificial neural networks, *Science* **355**, 602 (2017), <https://www.science.org/doi/pdf/10.1126/science.aag2302>.

[16] J. Hermann, Z. Schätzle, and F. Noé, Deep-neural-network solution of the electronic schrödinger equation, *Nature Chemistry* **12**, 891 (2020).

[17] D. Pfau, J. S. Spencer, A. G. D. G. Matthews, and W. M. C. Foulkes, Ab initio solution of the many-electron schrödinger equation with deep neural networks, *Phys. Rev. Research* **2**, 033429 (2020).

[18] N. Metropolis and S. Ulam, The monte carlo method, *Journal of the American Statistical Association* **44**, 335 (1949), pMID: 18139350, <https://www.tandfonline.com/doi/pdf/10.1080/01621459.1949.10483>.

[19] M. Troyer and U.-J. Wiese, Computational complexity and fundamental limitations to fermionic quantum monte carlo simulations, *Phys. Rev. Lett.* **94**, 170201 (2005).

[20] M. Marvian, D. A. Lidar, and I. Hen, On the computa-

tional complexity of curing non-stoquastic hamiltonians, *Nature Communications* **10**, 1571 (2019).

[21] J. Kolorenč and L. Mitas, Applications of quantum monte carlo methods in condensed systems, *Reports on Progress in Physics* **74**, 026502 (2011).

[22] B. M. Austin, D. Y. Zubarev, and W. A. Lester, Quantum monte carlo and related approaches, *Chemical Reviews* **112**, 263 (2012).

[23] A. Y. Kitaev, Quantum measurements and the abelian stabilizer problem, *arXiv preprint quant-ph/9511026* (1995).

[24] A. Y. Kitaev, A. Shen, M. N. Vyalyi, and M. N. Vyalyi, *Classical and quantum computation*, 47 (American Mathematical Soc., 2002).

[25] R. Babbush, C. Gidney, D. W. Berry, N. Wiebe, J. McClean, A. Paler, A. Fowler, and H. Neven, Encoding electronic spectra in quantum circuits with linear t complexity, *Phys. Rev. X* **8**, 041015 (2018).

[26] C. Gidney and M. Ekerå, How to factor 2048 bit rsa integers in 8 hours using 20 million noisy qubits, *Quantum* **5**, 433 (2021).

[27] S. McArdle, T. Jones, S. Endo, Y. Li, S. C. Benjamin, and X. Yuan, Variational ansatz-based quantum simulation of imaginary time evolution, *npj Quantum Information* **5**, 75 (2019).

[28] S. Endo, J. Sun, Y. Li, S. C. Benjamin, and X. Yuan, Variational quantum simulation of general processes, *Phys. Rev. Lett.* **125**, 010501 (2020).

[29] X. Yuan, S. Endo, Q. Zhao, Y. Li, and S. C. Benjamin, Theory of variational quantum simulation, *Quantum* **3**, 191 (2019).

[30] M. Motta, C. Sun, A. T. K. Tan, M. J. O'Rourke, E. Ye, A. J. Minnich, F. G. S. L. Brandão, and G. K.-L. Chan, Determining eigenstates and thermal states on a quantum computer using quantum imaginary time evolution, *Nature Physics* **16**, 205 (2020).

[31] H. Nishi, T. Kosugi, and Y.-i. Matsushita, Implementation of quantum imaginary-time evolution method on nisq devices by introducing nonlocal approximation, *npj Quantum Information* **7**, 85 (2021).

[32] A. Abbas, D. Sutter, C. Zoufal, A. Lucchi, A. Figalli, and S. Woerner, The power of quantum neural networks, *Nature Computational Science* **1**, 403 (2021).

[33] Y. Du, Z. Tu, X. Yuan, and D. Tao, An efficient measure for the expressivity of variational quantum algorithms (2021), *arXiv:2104.09961 [quant-ph]*.

[34] Z. Holmes, K. Sharma, M. Cerezo, and P. J. Coles, Connecting ansatz expressibility to gradient magnitudes and barren plateaus (2021), *arXiv:2101.02138 [quant-ph]*.

[35] Z. Holmes, A. Arrasmith, B. Yan, P. J. Coles, A. Albrecht, and A. T. Sornborger, Barren plateaus preclude learning scramblers, *Phys. Rev. Lett.* **126**, 190501 (2021).

[36] The framework also works even if the function is not strictly non-increasing.

[37] For any finite dimensional Hamiltonian, we can always shift it by a constant value to make it positive.

[38] Z.-J. Zhang, J. Sun, X. Yuan, and M.-H. Yung, Low-depth hamiltonian simulation by adaptive product formula, *arXiv preprint arXiv:2011.05283* (2020).

[39] *Quantum Information and Computation* **12**, 10.26421/qic12.11-12 (2012).

[40] D. W. Berry, A. M. Childs, R. Cleve, R. Kothari, and R. D. Somma, Simulating hamiltonian dynamics with a truncated taylor series, *Phys. Rev. Lett.* **114**, 090502 (2015).

[41] D.-B. Zhang, G.-Q. Zhang, Z.-Y. Xue, S.-L. Zhu, and Z. D. Wang, Continuous-variable assisted thermal quantum simulation, *Phys. Rev. Lett.* **127**, 020502 (2021).

[42] C. Y.-Y. Lin and Y. Zhu, Performance of qaoa on typical instances of constraint satisfaction problems with bounded degree, *arXiv preprint arXiv:1601.01744* (2016).

[43] Z. Wang, S. Hadfield, Z. Jiang, and E. G. Rieffel, Quantum approximate optimization algorithm for MaxCut: A fermionic view, *Phys. Rev. A* **97**, 022304 (2018).

[44] N. Moll, P. Barkoutsos, L. S. Bishop, J. M. Chow, A. Cross, D. J. Egger, S. Filipp, A. Fuhrer, J. M. Gambetta, M. Ganzhorn, *et al.*, Quantum optimization using variational algorithms on near-term quantum devices, *Quantum Science and Technology* **3**, 030503 (2018).

[45] C. Bravo-Prieto, R. LaRose, M. Cerezo, Y. Subasi, L. Cincio, and P. J. Coles, Variational quantum linear solver: A hybrid algorithm for linear systems, *arXiv preprint arXiv:1909.05820* (2019).

[46] X. Xu, J. Sun, S. Endo, Y. Li, S. C. Benjamin, and X. Yuan, Variational algorithms for linear algebra, *Science Bulletin* <https://doi.org/10.1016/j.scib.2021.06.023> (2021).

[47] H.-Y. Huang, K. Bharti, and P. Rebentrost, Near-term quantum algorithms for linear systems of equations, *arXiv preprint arXiv:1909.07344* (2019).

[48] S. Khatri, R. LaRose, A. Poremba, L. Cincio, A. T. Sornborger, and P. J. Coles, Quantum-assisted quantum compiling, *Quantum* **3**, 140 (2019).

[49] K. Heya, Y. Suzuki, Y. Nakamura, and K. Fujii, Variational quantum gate optimization, *arXiv preprint arXiv:1810.12745* (2018).

[50] T. Jones and S. C. Benjamin, Quantum compilation and circuit optimisation via energy dissipation, *arXiv preprint arXiv:1811.03147* (2018).

[51] K. Sharma, S. Khatri, M. Cerezo, and P. J. Coles, Noise resilience of variational quantum compiling, *New Journal of Physics* **22**, 043006 (2020).

[52] J. Carolan, M. Mohseni, J. P. Olson, M. Prabhu, C. Chen, D. Bunandar, M. Y. Niu, N. C. Harris, F. N. Wong, M. Hochberg, *et al.*, Variational quantum unsampling on a quantum photonic processor, *Nature Physics* **16**, 322–327 (2020).

[53] P. D. Johnson, J. Romero, J. Olson, Y. Cao, and A. Aspuru-Guzik, Qvector: an algorithm for device-tailored quantum error correction, *arXiv preprint arXiv:1711.02249* (2017).

[54] X. Xu, S. C. Benjamin, and X. Yuan, Variational circuit compiler for quantum error correction, *Phys. Rev. Applied* **15**, 034068 (2021).

[55] We note that the argument assumes a large τ independent of the measurement accuracy. However, when the gap between the ground and the first excited state is finite, as happens in satisfactory problems, linear algebra tasks, and quantum state compiling, we only need to choose $\tau = \mathcal{O}(\log(1/\varepsilon))$ as a logarithmic function of the state infidelity ε (when $g(h)$ is exponential, Gaussian, or hyperbolic). Then the numerator $N_\tau(\psi_0, O)$ and denominator $D_\tau(\psi_0)$ scales as $\mathcal{O}(\text{poly}(1/\varepsilon))$ and the sample complexity will not be exponentially large.

[56] B. Bauer, D. Wecker, A. J. Millis, M. B. Hastings, and M. Troyer, Hybrid quantum-classical approach to correlated materials, *Physical Review X* **6**, 031045 (2016).

[57] Y. Cao, J. Romero, J. P. Olson, M. Degroote, P. D. Johnson, M. Kieferová, I. D. Kivlichan, T. Menke, B. Peropadre, N. P. Sawaya, *et al.*, Quantum chemistry in the age of quantum computing, *Chemical reviews* **119**, 10856 (2019).

[58] S. McArdle, S. Endo, A. Aspuru-Guzik, S. C. Benjamin, and X. Yuan, Quantum computational chemistry, *Reviews of Modern Physics* **92**, 015003 (2020).

[59] B. Bauer, S. Bravyi, M. Motta, and G. K.-L. Chan, Quantum algorithms for quantum chemistry and quantum materials science, *Chemical Reviews* **120**, 12685 (2020).

[60] M. Motta and J. Rice, Emerging quantum computing algorithms for quantum chemistry (2021), arXiv:2109.02873 [quant-ph].

[61] X. Yuan, J. Sun, J. Liu, Q. Zhao, and Y. Zhou, Quantum simulation with hybrid tensor networks, *Phys. Rev. Lett.* **127**, 040501 (2021).

[62] S. Endo, Z. Cai, S. C. Benjamin, and X. Yuan, Hybrid quantum-classical algorithms and quantum error mitigation, *Journal of the Physical Society of Japan* **90**, 032001 (2021), <https://doi.org/10.7566/JPSJ.90.032001>.

[63] M. Cerezo, A. Arrasmith, R. Babbush, S. C. Benjamin, S. Endo, K. Fujii, J. R. McClean, K. Mitarai, X. Yuan, L. Cincio, and P. J. Coles, Variational quantum algorithms, *Nature Reviews Physics* **3**, 625 (2021).

[64] K. Bharti, A. Cervera-Lierta, T. H. Kyaw, T. Haug, S. Alperin-Lea, A. Anand, M. Degroote, H. Heimonen, J. S. Kottmann, T. Menke, W.-K. Mok, S. Sim, L.-C. Kwek, and A. Aspuru-Guzik, Noisy intermediate-scale quantum (nisq) algorithms (2021), arXiv:2101.08448 [quant-ph].

[65] S. Lu, M. C. Bañuls, and J. I. Cirac, Algorithms for quantum simulation at finite energies, *PRX Quantum* **2**, 020321 (2021).

[66] S. Endo, J. Sun, Y. Li, S. C. Benjamin, and X. Yuan, Variational quantum simulation of general processes, *Phys. Rev. Lett.* **125**, 010501 (2020).

[67] M. Huo and Y. Li, Shallow trotter circuits fulfil error-resilient quantum simulation of imaginary time (2021), arXiv:2109.07807 [quant-ph].

[68] G. K. Karagiannidis and A. S. Lioumpas, An improved approximation for the gaussian q-function, *IEEE Communications Letters* **11**, 644 (2007).

Appendix A: Cooling functions and the dual phase representations

In this work, we consider an n -qubit system with a gapped Hamiltonian H . The eigenstate $|u_i\rangle$ and the corresponding eigenenergy E_i of the Hamiltonian satisfy,

$$H|u_i\rangle = E_i|u_i\rangle, \quad i = 0, 1, \dots, N-1. \quad (\text{A1})$$

Here, $N := 2^n$.

We define the cooling function $g(h)$ as follows.

Definition 1. A real-valued function $g(h) : \mathbb{R} \rightarrow \mathbb{R}$ is called a cooling function if it satisfies,

1. The value of $g(0)$ is non-zero: $g(0) \neq 0$;
2. The absolute value of $g(h)$ is a single peak shape: $g(h') \leq g(h)$, $\forall h' > h > 0$ and $\forall h' < h < 0$;
3. The asymptotic value of $h \neq 0$ is vanishing: $\lim_{\tau \rightarrow \infty} \left| \frac{g(\tau h)}{g(0)} \right| = 0$, $\forall h \neq 0$.

For a given n -qubit Hamiltonian, suppose we want to prepare the j -th eigenstate $|u_j\rangle$ with eigenenergy E_j . We define a cooling operator as follows,

$$g(\tau(H - E_j)) := \sum_{i=0}^{N-1} g(\tau(E_i - E_j)) |u_i\rangle \langle u_i|. \quad (\text{A2})$$

Then, for any given initial state $|\psi_0\rangle$ with $|\langle\psi_0|u_j\rangle|^2 \neq 0$, the cooling operator evolve $|\psi_0\rangle$ to the eigenstate $|u_j\rangle$,

$$\lim_{\tau \rightarrow \infty} g(\tau(H - E_j)) |\psi_0\rangle \propto |u_j\rangle. \quad (\text{A3})$$

The cooling operator is usually a nonphysical operation. To realize it, we consider its dual realization based on a Fourier transform,

$$\begin{aligned} f(x) &= \int_{-\infty}^{\infty} g(h) e^{-ixh} dh, \\ g(h) &= \frac{1}{2\pi} \int_{-\infty}^{\infty} f(x) e^{ixh} dx. \end{aligned} \quad (\text{A4})$$

We define the norm of the dual function $f(x)$ as

$$\|f\| := \int_{-\infty}^{\infty} |f(x)| dx, \quad (\text{A5})$$

Suppose $\|f\|$ is finite, we can decompose $f(x)$ to a normalized probability distribution with an extra phase,

$$f(x) = |f(x)| e^{i\phi(x)} = \|f\| p(x) e^{i\phi(x)}. \quad (\text{A6})$$

The Fourier transform in Eq. (A4) can then be re-written as

$$\begin{aligned} p(x) &= \frac{1}{\|f\|} \int_{-\infty}^{\infty} g(h) e^{-i\phi(x)} e^{-ixh} dh, \\ g(h) &= \frac{\|f\|}{2\pi} \int_{-\infty}^{\infty} p(x) e^{i\phi(x)} e^{ixh} dx. \end{aligned} \quad (\text{A7})$$

Based on Eq. (A7), the cooling operator $g(\tau(H - E_j))$ in Eq. (A2) can be expanded as,

$$\begin{aligned} g(\tau(H - E_j)) &= \frac{\|f\|}{2\pi} \int_{-\infty}^{\infty} p(x) e^{i\phi(x)} e^{ix\tau(H - E_j)} dx, \\ &= \frac{\|f\|}{2\pi} \int_{-\infty}^{\infty} p(x) e^{i(\phi(x) - \tau x E_j)} e^{i\tau x H} dx. \end{aligned} \quad (\text{A8})$$

Therefore, to realize a quantum cooling operator $g(\tau(H - E_j))$, we can expand it to a weighted superposition of the unitary operators e^{itH} with different evolution time $t = \tau x$ ranging from $-\infty$ to ∞ .

In practice, the evolution time is a limited number related to the depth of the quantum circuit. We define the truncated cooling function as,

$$\tilde{g}(h; x_m) = \frac{\|f\|}{2\pi} \int_{-x_m}^{x_m} p(x) e^{i\phi(x)} e^{ixh} dx. \quad (\text{A9})$$

The difference of the $\tilde{g}(h; x_m)$ from $g(h)$ is bounded by

$$\begin{aligned} |g(h) - \tilde{g}(h; x_m)| &= \frac{\|f\|}{2\pi} \left| \int_{-\infty}^{-x_m} p(x) e^{i\phi(x)} e^{ixh} dx + \int_{x_m}^{\infty} p(x) e^{i\phi(x)} e^{ixh} dx \right| \\ &\leq \frac{\|f\|}{2\pi} \int_{-\infty}^{-x_m} |p(x) e^{i\phi(x)} e^{ixh}| dx + \int_{x_m}^{\infty} |p(x) e^{i\phi(x)} e^{ixh}| dx \\ &= \frac{\|f\|}{2\pi} \left(1 - \int_{-x_m}^{x_m} p(x) dx \right). \end{aligned} \quad (\text{A10})$$

Later in Sec. C we will show that, the estimation error caused by the finite evolution time will be bounded by the tail probability of $p(x)$.

Definition 2. We say a cooling function $g(h)$ in Definition 1 is realizable if the following requirements hold.

C0. The Fourier transform of $g(h)$ exists,

$$f(x) = \int_{-\infty}^{\infty} g(h) e^{-ixh} dh. \quad (\text{A11})$$

C1. The norm of the dual function $\|f\|$

$$\|f\| := \int_{-\infty}^{\infty} |f(x)| dx, \quad (\text{A12})$$

is finite.

C2. $\left| 1 - \int_{-L(\varepsilon)}^{L(\varepsilon)} p(x) dx \right| \leq \varepsilon$, $\forall \varepsilon \geq 0$, $\exists L(\varepsilon) = \mathcal{O}(\text{poly}(\frac{1}{\varepsilon}))$.

Now, we introduce several typical cooling functions and discuss their properties.

1. Rectangular function

The rectangular function $\text{rect}(h)$ is defined as,

$$\text{rect}(h) = \begin{cases} 1, & |h| \leq \frac{1}{2}, \\ 0, & |h| > \frac{1}{2}. \end{cases} \quad (\text{A13})$$

It satisfies Definition 1 and hence a cooling function. When acting as a cooling function $g(\tau(H - E_j))$, the rectangular function is an ideal ‘‘energy band filter’’, as it projects the state to the energy subspace in the range $[E_j - \frac{1}{2\tau}, E_j + \frac{1}{2\tau}]$.

The Fourier transform of $\text{rect}(h)$ is the Sinc function,

$$f(x) = \text{sinc}\left(\frac{x}{2\pi}\right), \quad (\text{A14})$$

where $\text{sinc}(x) := \frac{\sin x}{x}$.

Unfortunately, the norm of $f(x)$ is infinite,

$$\begin{aligned}
\|f\| &= \int_{-\infty}^{\infty} |\text{sinc}\left(\frac{x}{2\pi}\right)| \\
&= 4\pi \int_0^{\infty} |\text{sinc}y| dy \\
&= 4\pi \sum_{k=0}^{\infty} \int_{k\pi}^{(k+1)\pi} \left| \frac{\sin y}{y} \right| dy \\
&> 4\pi \sum_{k=0}^{\infty} \int_{k\pi}^{(k+1)\pi} \frac{|\sin y|}{(k+1)\pi} dy \\
&= 4\pi \sum_{k=0}^{\infty} \frac{1}{k+1}.
\end{aligned} \tag{A15}$$

From the divergence of $\sum_{k=0}^{\infty} \frac{1}{k+1}$ we know that $\|f\| = \infty$. As a result, the rectangular function is not a realizable cooling function based on Definition 2.

2. Triangular function

The triangular function $\text{tri}(h)$ is defined as,

$$\text{tri}(h) = \begin{cases} 1 - |h|, & |h| \leq 1, \\ 0, & |h| > 1. \end{cases} \tag{A16}$$

It satisfies Definition 1 and hence a cooling function. Similar to the rectangular function, it can be used as an “energy band filter”, since it filters the energy in the range $[E_j - \frac{1}{\tau}, E_j + \frac{1}{\tau}]$. However, it will modify the weight of different energy values in that range. When $h \geq 0$, the inverse function of $\text{tri}(h)$ is

$$g^{-1}(p) = 1 - p \leq 1. \tag{A17}$$

The Fourier transform of $\text{rect}(h)$ is the square of Sinc function,

$$f(x) = \text{sinc}^2\left(\frac{x}{2\pi}\right). \tag{A18}$$

The norm of $f(x)$ is finite,

$$\|f\| = 2\pi \int_{-\infty}^{\infty} \text{sinc}^2(y) dy = 2\pi^2. \tag{A19}$$

The sample probability distribution is then,

$$p(x) = \frac{1}{\|f\|} f(x) = \frac{1}{2\pi^2} \text{sinc}^2\left(\frac{x}{2\pi}\right). \tag{A20}$$

To check the realizability of cooling function $g(h)$, we need to study the property of the tail probability of $p(x)$ with respect to the cutoff sample time x_m . Solving the following equation,

$$\varepsilon = \int_{-x_m}^{x_m} p(x) dx, \tag{A21}$$

where $p(x)$ is defined in Eq. (A20), we have

$$\varepsilon = \frac{2}{\pi} \left(\frac{\pi}{2} - \text{Si}\left(\frac{x_m}{\pi}\right) \right) + \frac{2 - 2 \cos\left(\frac{x_m}{\pi}\right)}{x_m}, \tag{A22}$$

where $\text{Si}(x) := \int_0^x \text{sinc}(y) dy$ is the Sinc integral function. Now we proven that,

$$\frac{\pi}{2} - \text{Si}(x) \leq \frac{1}{x}. \tag{A23}$$

Proof. We have,

$$\frac{\pi}{2} - \text{Si}(x) = \int_x^\infty \frac{\sin(t)}{t} dt = \int_x^\infty \frac{\cos x \sin(t-x) + \sin x \cos(t-x)}{t} dt. \quad (\text{A24})$$

Now we denote $f(t) = \sin x \cos t + \cos x \sin t$, then

$$\frac{\pi}{2} - \text{Si}(x) = \int_x^\infty \frac{f(t-x)}{t} dt. \quad (\text{A25})$$

We introduce the Laplace transform of $f(t)$,

$$\mathcal{L}[f(t)](s) = \int_0^\infty f(t) e^{-st} dt, \quad (\text{A26})$$

then,

$$\frac{\pi}{2} - \text{Si}(x) = \mathcal{L} \left[\frac{f(t-x)u(t-x)}{t} \right] (0), \quad (\text{A27})$$

where $u(t) := \eta(t \geq 0)$.

From the property of Laplace transform, we have

$$\begin{aligned} \int_s^\infty \mathcal{L}[f(t)](p) e^{-xp} dp &= \int_s^\infty \mathcal{L}[f(t-x)u(t-x)](p) e^{-xp} dp \\ &= \mathcal{L} \left[\frac{f(t-x)u(t-x)}{t} \right] (s). \end{aligned} \quad (\text{A28})$$

On the other hand, we know that

$$\mathcal{L}[f(t)](p) = \mathcal{L}[\sin x \cos t + \cos x \sin t](p) = \frac{\sin x p + \cos x}{p^2 + 1}, \quad (\text{A29})$$

then

$$\int_s^\infty \mathcal{L}[f(t)](p) e^{-xp} dp = \int_s^\infty \frac{\sin x p + \cos x}{p^2 + 1} e^{-xp} dp. \quad (\text{A30})$$

Taking $s = 0$ and combine Eq. (A27), (A28), and (A30), we have

$$\frac{\pi}{2} - \text{Si}(x) = \int_0^\infty \frac{\sin x p + \cos x}{p^2 + 1} e^{-xp} dp. \quad (\text{A31})$$

Using Cauchy-Schwarz inequality we can prove that,

$$p \sin x + 1 \cdot \cos x \leq \sqrt{1 + p^2} \sqrt{\sin^2 x + \cos^2 x} = \sqrt{1 + p^2}, \quad (\text{A32})$$

hence

$$\begin{aligned} \frac{\pi}{2} - \text{Si}(x) &= \int_0^\infty \frac{\sin x p + \cos x}{p^2 + 1} e^{-xp} dp \\ &\leq \int_0^\infty \frac{1}{\sqrt{p^2 + 1}} e^{-xp} dp \\ &\leq \int_0^\infty e^{-xp} dp \\ &= \frac{1}{x}. \end{aligned} \quad (\text{A33})$$

□

Therefore,

$$\begin{aligned}\varepsilon &\leq \frac{2}{\pi} \frac{\pi}{x_m} + \frac{2 - 2 \cos(\frac{x_m}{\pi})}{x_m} \\ &\leq \frac{2}{x_m} + \frac{4}{x_m} = \frac{6}{x_m}.\end{aligned}\tag{A34}$$

We have

$$x_m \leq \frac{6}{\varepsilon} =: L(\varepsilon) = \mathcal{O}(\text{poly}(\frac{1}{\varepsilon})).\tag{A35}$$

Therefore, the triangle function is a realizable cooling function. However, the circuit depth requirement of triangle function is still demanding, as the tail probability ε decays slowly with the cutoff time x_m .

3. Double-side exponential decay function

The double-side exponential decay function is

$$g(h) := e^{-|h|}.\tag{A36}$$

Hereafter we call it exponential function for simplicity. It satisfies Definition 1 and hence a cooling function. The exponential function is of special importance as it describes the imaginary time evolution $e^{-\tau H}$ when the eigenenergies are all positive. When $h \geq 0$, the inverse function is

$$g^{-1}(p) = \ln(\frac{1}{p}).\tag{A37}$$

The Fourier transform of the exponential function is

$$f(x) = \frac{2}{1+x^2}.\tag{A38}$$

The norm of $f(x)$ is finite,

$$\|f\| = \int_{-\infty}^{\infty} \frac{2}{1+x^2} dx = 2\pi.\tag{A39}$$

The sample probability distribution is,

$$p(x) = \frac{1}{\|f\|} f(x) = \frac{1}{2\pi} \frac{2}{1+x^2},\tag{A40}$$

which is a Lorentzian distribution.

Now, we check the tail probability of $p(x)$ with respect to the cutoff sample time x_m . Solving the following equation,

$$\varepsilon = \int_{-x_m}^{x_m} p(x) dx,\tag{A41}$$

where $p(x)$ is defined in Eq. (A40), we have

$$x_m = \tan\left[\frac{\pi}{2}(1-\varepsilon)\right],\tag{A42}$$

To calculate the dependence of x_m with respect to $\frac{1}{\varepsilon}$, we expand $\frac{1}{x_m}$ at the point $\varepsilon \rightarrow 0^+$ using Taylor expansion with remainder,

$$\begin{aligned}\frac{1}{x_m} &= \frac{1}{\tan\left[\frac{\pi}{2}(1-\varepsilon)\right]} \\ &= 0 + \frac{\pi}{2} \frac{1}{\cos^2(\frac{\pi}{2} \cdot 0)} \varepsilon + \frac{\pi^2}{4} \frac{\sin(\pi\xi)}{\cos^4(\frac{\pi}{2}\xi)} \frac{\varepsilon^2}{2} \\ &> \frac{\pi}{2} \varepsilon,\end{aligned}\tag{A43}$$

where $\xi \in (0, \varepsilon)$. We then have,

$$x_m < \frac{2}{\pi} \frac{1}{\varepsilon} =: L(\varepsilon) = \mathcal{O}(\text{poly}(\frac{1}{\varepsilon})). \quad (\text{A44})$$

Therefore, the exponential function is a realizable cooling function. Still, the circuit depth requirement is demanding, as the tail probability ε decays slowly with the cutoff time x_m . In what follows, we consider two cooling functions with small tails.

4. Gaussian function

The Gaussian function we used here is

$$g(h) := e^{-h^2}. \quad (\text{A45})$$

It satisfies Definition 1 and hence a cooling function. When $h \geq 0$, the inverse function is

$$g^{-1}(p) = \sqrt{\ln(\frac{1}{p})}. \quad (\text{A46})$$

The Fourier transform of Gaussian function is still a Gaussian function,

$$f(x) = \sqrt{\pi} e^{-\frac{x^2}{4}}. \quad (\text{A47})$$

The norm of $f(x)$ is finite,

$$\|f\| = \sqrt{\pi} \int_{-\infty}^{\infty} e^{-\frac{x^2}{4}} dx = 2\pi. \quad (\text{A48})$$

The sample probability distribution is,

$$p(x) = \frac{1}{\|f\|} f(x) = \frac{1}{2\pi} \sqrt{\pi} e^{-\frac{x^2}{4}}, \quad (\text{A49})$$

which is a Gaussian distribution.

Now, we check the tail probability of $p(x)$ with respect to the cutoff sample time x_m . Solving the following equation,

$$\varepsilon = \int_{-x_m}^{x_m} p(x) dx, \quad (\text{A50})$$

where $p(x)$ is defined in Eq. (A49), we have

$$\varepsilon = \text{erfc}(\frac{x_m}{2}), \quad (\text{A51})$$

where $\text{erfc}(x) := 1 - \frac{2}{\sqrt{\pi}} \int_0^x e^{-t^2} dt$ is the complementary of the error function. It can be upper-bounded by a Chernoff-type formula [68],

$$\text{erfc}(x) \leq \frac{1}{\sqrt{\pi}x} e^{-x^2}, \quad x \geq 0. \quad (\text{A52})$$

Therefore,

$$\begin{aligned} \varepsilon &= \text{erfc}(\frac{x_m}{2}) \leq \frac{2}{\sqrt{\pi}x_m} e^{-\frac{x_m^2}{4}} \\ \Rightarrow \quad \ln \frac{\sqrt{\pi}\varepsilon}{2} &\leq -\frac{x_m^2}{4} - \ln x_m \\ \Rightarrow \quad \frac{x_m^2}{4} &\leq \frac{x_m^2}{4} + \ln x_m \leq -\ln \left(\frac{\sqrt{\pi}\varepsilon}{2} \right) \\ \Rightarrow \quad x_m &\leq 2\sqrt{-\ln \varepsilon - \ln \frac{\sqrt{\pi}}{2}} \leq 2\sqrt{\ln \left(\frac{1}{\varepsilon} \right)}. \end{aligned} \quad (\text{A53})$$

We have $L(\varepsilon) = 2\sqrt{\ln(\frac{1}{\varepsilon})} = \mathcal{O}(\text{poly}(\frac{1}{\varepsilon}))$. Therefore, the Gaussian function is a realizable cooling function. Note that, unlike the triangular function or the exponential function, the tail of Gaussian function decays quickly with respect to x_m . This implies that the Gaussian cooling is more experimentally friendly.

5. Secant hyperbolic function

The secant hyperbolic function is

$$\operatorname{sech}(h) := \frac{2}{e^h + e^{-h}}. \quad (\text{A54})$$

It satisfies Definition 1 and hence a cooling function. The inverse of sech is hard to be presented in an analytical form, but we can easily derive an upper bound for it,

$$g^{-1}(h) < \ln \frac{2}{p}. \quad (\text{A55})$$

The Fourier transform of secant hyperbolic function is still a secant hyperbolic function,

$$f(x) = \pi \operatorname{sech}\left(\frac{\pi}{2}x\right). \quad (\text{A56})$$

The norm of $f(x)$ is finite,

$$\|f\| = \pi \int_{-\infty}^{\infty} \operatorname{sech}\left(\frac{\pi}{2}x\right) dx = 2\pi. \quad (\text{A57})$$

The sample probability distribution is,

$$p(x) = \frac{1}{\|f\|} f(x) = \frac{1}{2\pi} \pi \operatorname{sech}\left(\frac{\pi}{2}x\right), \quad (\text{A58})$$

which is a secant hyperbolic distribution.

Now, we check the tail probability of $p(x)$ with respect to the cutoff sample time x_m . Solving the following equation,

$$\varepsilon = \int_{-x_m}^{x_m} p(x) dx, \quad (\text{A59})$$

where $p(x)$ is defined in Eq. (A58), we have

$$\begin{aligned} x_m &= \frac{2}{\pi} \ln \left\{ \tan \left[\frac{\pi}{2} \left(1 - \frac{\varepsilon}{2} \right) \right] \right\} \\ \Rightarrow e^{-\frac{\pi}{2}x_m} &= \frac{1}{\tan \left[\frac{\pi}{2} \left(1 - \frac{\varepsilon}{2} \right) \right]}. \end{aligned} \quad (\text{A60})$$

Similar to Eq. (A43), we expand the inversed tangent function at the point $\varepsilon \rightarrow 0^+$ using Taylor expansion with remainder,

$$\begin{aligned} e^{-\frac{\pi}{2}x_m} &= \frac{1}{\tan \left[\frac{\pi}{2} \left(1 - \frac{\varepsilon}{2} \right) \right]} \\ &= 0 + \frac{\pi}{4} \frac{1}{\cos^2(\frac{\pi}{4} \cdot 0)} \varepsilon + \pi^2 \frac{\sin^4(\frac{\pi}{4}\xi)}{\sin^3(\frac{\pi}{2}\xi)} \frac{\varepsilon^2}{2} \\ &> \frac{\pi}{4} \varepsilon, \end{aligned} \quad (\text{A61})$$

where $\xi \in (0, \varepsilon)$. Therefore,

$$x_m < \frac{2}{\pi} \ln \left(\frac{4}{\pi} \frac{1}{\varepsilon} \right) =: L(\varepsilon) = \mathcal{O}(\operatorname{poly}(\frac{1}{\varepsilon})). \quad (\text{A62})$$

Therefore, the secant hyperbolic function is also a realizable function. The overhead of secant hyperbolic function is better then the Gaussian function; however, the asymptotic cost of the Gaussian function is quadratically better then the secant hyperbolic function.

Appendix B: Detailed quantum cooling algorithm

Suppose we want to estimate the expectation value $\langle O \rangle := \langle u_j | O | u_j \rangle$ using the quantum cooling algorithm. For a given finite evolution time τ , the estimation value of $\langle O \rangle_{\psi(\tau)}$ is given by

$$\langle O \rangle_{\psi(\tau)} = \frac{N_\tau(\psi_0, O)}{D_\tau(\psi_0)}, \quad (\text{B1})$$

where

$$D_\tau(\psi_0) = \langle \psi_0 | g^2(\tau(H - E_j)) | \psi_0 \rangle, \quad N_\tau(\psi_0, O) = \langle \psi_0 | g(\tau(H - E_j)) O g(\tau(H - E_j)) | \psi_0 \rangle. \quad (\text{B2})$$

are, respectively, the normalization factor and the unnormalized expectation value. Using Eq. (A8), we expand the cooling operator $g(\tau(H - E_j))$ and receive the following estimation formulas,

$$\begin{aligned} D_\tau(\psi_0) &= \left(\frac{\|f\|}{2\pi} \right)^2 \int_{-\infty}^{\infty} dy \tilde{p}(y) e^{-i\tau y E_j} \langle \psi_0 | e^{i\tau y H} | \psi_0 \rangle, \\ N_\tau(\psi_0, O) &= \left(\frac{\|f\|}{2\pi} \right)^2 \int_{-\infty}^{\infty} dx \int_{-\infty}^{\infty} dx' p(x) p(x') \sum_{l \in \mathcal{P}_n} o_l e^{-i\tau(x-x') E_j} \langle \psi_0 | e^{-i\tau x' H} P_l e^{i\tau x' H} | \psi_0 \rangle, \end{aligned} \quad (\text{B3})$$

where $\tilde{p}(y) := \frac{1}{2} \int_{-\infty}^{\infty} p\left(\frac{z+y}{2}\right) p\left(\frac{z-y}{2}\right) dz$ is the self-correlation of the probability $p(x)$. We remark that, the normalization factor $\left(\frac{\|f\|}{2\pi} \right)^2$ can be removed, since it is the same for both $D_\tau(\psi_0)$ and $N_\tau(\psi_0, O)$, hence independent of the estimation of $\langle O \rangle_{\psi(\tau)}$. In the following discussion, we ignore this normalization factor during the estimation procedure.

In the quantum cooling algorithm, we generate the (normalized) evolution time x (or y) based on the sample probability $p(x)$ (or $\tilde{p}(y)$) and sample the innerproduct values using quantum experiments. For a practical consideration, when the (normalized) evolution time x (or y) is larger then a cutoff value x_m , we don't perform the quantum experiment and direct denote the estimation of this round to be 0. In this way, the estimation formula of $N_\tau(\psi_0, O)$ and $D_\tau(\psi_0)$, originally given by Eq. (B3), now becomes

$$\begin{aligned} D_\tau^{x_m}(\psi_0) &= \int_{-x_m}^{x_m} dy \tilde{p}(y) e^{-i\tau y E_j} \langle \psi_0 | e^{i\tau y H} | \psi_0 \rangle, \\ N_\tau^{x_m}(\psi_0, O) &= \int_{-x_m}^{x_m} dx \int_{-x_m}^{x_m} dx' p(x) p(x') \sum_{l \in \mathcal{P}_n} o_l e^{-i\tau(x-x') E_j} \langle \psi_0 | e^{-i\tau x' H} P_l e^{i\tau x' H} | \psi_0 \rangle. \end{aligned} \quad (\text{B4})$$

To estimate the values of $N_\tau^{x_m}(\psi_0, O)$ and $D_\tau^{x_m}(\psi_0)$ in Eq. (B4), the core issue is to realize the unbiased estimation of the following quantities,

$$\begin{aligned} &\langle \psi_0 | e^{i\tau y H} | \psi_0 \rangle, \\ &\langle \psi_0 | e^{-i\tau x' H} P_l e^{i\tau x' H} | \psi_0 \rangle. \end{aligned} \quad (\text{B5})$$

These $\langle \psi | U | \psi \rangle$ form quantities can be estimated using the Hadamard test, shown in Fig. 3. To measure $\langle \psi | U | \psi \rangle$, we first prepare the state $|\psi\rangle$ and an extra ancillary qubit prepared on $|+\rangle$. Afterward, we perform a $C-U$ gate from ancillary to $|\psi\rangle$. If we directly measure the ancillary qubit on the X -basis, the outcome a will be 0 with a probability of $\frac{1}{2}(1 + \text{Re}(\langle \psi | U | \psi \rangle))$ and 1 with a probability of $\frac{1}{2}(1 - \text{Re}(\langle \psi | U | \psi \rangle))$. Alternatively, if we perform an extra S gate before the X -basis measurement, the outcome a will be 0 with a probability of $\frac{1}{2}(1 + \text{Im}(\langle \psi | U | \psi \rangle))$ and 1 with a probability of $\frac{1}{2}(1 - \text{Im}(\langle \psi | U | \psi \rangle))$.

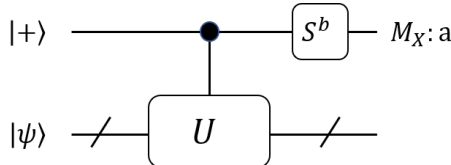


FIG. 3. The diagram of the Hadamard test. If $b = 0$, $\text{Pr}(a = 0) = \frac{1}{2}(1 + \text{Re}(\langle \psi | U | \psi \rangle))$; if $b = 1$, $\text{Pr}(a = 0) = \frac{1}{2}(1 + \text{Im}(\langle \psi | U | \psi \rangle))$.

Algorithm 1 Normalization factor estimation

Input: An n -qubit Hamiltonian H ; initial state $|\psi_0\rangle$ with nonzero overlap with j -th eigenstate of H : $p_j = |\langle u_j | \psi_0 \rangle|^2$; the energy E_j for the j -th eigenstate; cooling function $g(h)$ and the corresponding sampling probability $p(x)$; proper choice of the imaginary time τ , normalized cutoff time x_m .

Output: Estimation of the normalization factor $D_\tau(\psi_0)$.

```

1: for  $p = 1$  to  $N_M$  do
2:   Sample a normalized evolution time  $y_p$  from  $\tilde{p}(y) := \frac{1}{2} \int_{-\infty}^{\infty} p(\frac{z+y}{2})p(\frac{z-y}{2})dz$ .
3:   if  $y_p > x_m$  then ▷ Exceed the preset cutoff value
4:     Set the estimation  $\hat{d}_p = 0$ .
5:   else ▷ Normal single-shot quantum sampling by Hadamard test
6:     Prepare an ancillary qubit on  $|+\rangle$  state and the initial state  $|\psi_0\rangle$ .
7:     Implement a controlled-unitary  $C-U$  from the ancillary qubit to the state  $|\psi_0\rangle$ . Here,  $U = e^{i\tau y_p H}$ .
8:     Generate a random bit  $b_p$  with a even distribution of values 0/1. Perform a gate  $S^{b_p}$  on the ancillary qubit. Here,  $S = \text{diag}(1, -i)$  is a  $\frac{\pi}{4}$ -rotation gate.
9:     Measure the ancillary qubit on  $X$ -basis, and record the binary result  $a_p$ . Then record the values  $\{y_p, b_p, a_p\}$  and set the estimation value  $\hat{d}_p := 2(-1)^{a_p} i^{b_p} e^{-i\tau y_p E_j}$ .
10:  end if
11: end for
12: Calculate the estimated normalization factor  $\hat{D}_\tau(\psi_0) := \text{Re} \left( \frac{1}{N_M} \sum_{p=1}^{N_M} \hat{d}_p \right)$ .

```

To simplify the theoretical analysis, we now introduce a combined estimation of the real part and imaginary part in a single round. In each round of experiment, we first randomly decide the binary value b in Fig. 3. Based on the measurement outcome a , we construct the following complex-valued estimator,

$$\hat{r} = \begin{cases} 2, & (b, a) = (0, 0), \\ -2, & (b, a) = (0, 1), \\ 2i, & (b, a) = (1, 0), \\ -2i, & (b, a) = (1, 1). \end{cases} \quad (\text{B6})$$

In this case, $\mathbb{E}(\hat{r}) = \langle \psi | U | \psi \rangle$. In what follows, we consider a single-shot version of Hadamard test: each time we sample a x and perform the quantum experiment only once. This is for the simplicity of the theoretical analysis in Appendix C3.

In the main text, we consider two applications of the universal cooling: 1) to estimate the ground state properties when the ground state energy E_0 is known; 2) to estimate the properties of the j -th eigenstate without the exact knowledge of the energy. We can divide it to three elementary tasks:

1. Estimate the eigenenergy E_j of the j -th eigenstate given a initial guess interval $[E_j^L, E_j^U]$;
2. Given a known eigenenergy E_j , estimate the normalization factor $D_\tau(\psi_0)$;
3. Given a known eigenenergy E_j and an observable O , estimate the normalization factor $N_\tau(\psi_0, O)$.

We now introduce the detailed algorithm for these tasks.

1. Estimate the normalization factor

In Algorithm 1, we first introduce the algorithm to estimate the normalization factor $D_\tau(\psi_0)$ based on Eq. (B4) and the Hadamard test, when the eigenenergy E_j is known.

2. Estimate the eigenenergy

Suppose the initial state $|\psi_0\rangle$ has a constant overlap with the eigenstate $|u_j\rangle$. Then we can sweep the parameter $E_j^{(e)}$ in a range to maximize $D_\tau(\psi_0)$. The accuracy depends on the overlap p_j .

Algorithm 2 eigenenergy and normalization factor estimation

Input: An n -qubit Hamiltonian H ; initial state $|\psi_0\rangle$ with nonzero overlap with j -th eigenstate of H : $p_j = |\langle u_j | \psi_0 \rangle|^2$; the energy interval $[E_j^L, E_j^U]$ for the j -th eigenstate; cooling function $g(h)$ and the corresponding sampling probability $p(x)$; proper choice of the imaginary time τ , normalized cutoff time x_m .

Output: Estimation of the eigenenergy E_j and the corresponding normalization factor $\hat{D}_\tau(\psi_0)$.

```

1: for  $p = 1$  to  $N_M$  do
2:   Sample a normalized evolution time  $y_p$  from  $\tilde{p}(y) := \frac{1}{2} \int_{-\infty}^{\infty} p(\frac{z+y}{2})p(\frac{z-y}{2})dz$ .
3:   if  $y_p > x_m$  then ▷ Exceed the preset cutoff value
4:     Set the estimation  $\hat{d}_p = 0$ .
5:   else ▷ Normal single-shot quantum sampling by Hadamard test
6:     Prepare an ancillary qubit on  $|+\rangle$  state and the initial state  $|\psi_0\rangle$ .
7:     Implement a controlled-unitary  $C-U$  from the ancillary qubit to the state  $|\psi_0\rangle$ . Here,  $U = e^{i\tau y_p H}$ .
8:     Generate a random bit  $b_p$  with a even distribution of values 0/1. Perform a gate  $S^{b_p}$  on the ancillary qubit. Here,  $S = \text{diag}(1, -i)$  is a  $\frac{\pi}{4}$ -rotation gate.
9:     Measure the ancillary qubit on  $X$ -basis, and record the binary result  $a_p$ . Then record the values  $\{y_p, b_p, a_p\}$  and set the temporal estimation value  $\hat{d}_p := 2(-1)^{a_p} i^{b_p}$ .
10:  end if
11: end for
12: Set the estimated normalization factor  $\hat{D}_\tau(\psi_0)' = 0$ .
13: for  $E'_j$  in  $[E_j^L, E_j^U]$  do ▷ Try different possible eigenenergy value
14:   Calculate the estimated normalization factor  $\hat{D}_\tau(\psi_0)' := \text{Re} \left( \frac{1}{N_M} \sum_{p=1}^{N_M} e^{-i\tau y_p E'_j} \hat{d}_p \right)$ .
15:   if  $\hat{D}_\tau(\psi_0)' > \hat{D}_\tau(\psi_0)$  then
16:     Set  $\hat{D}_\tau(\psi_0) = \hat{D}_\tau(\psi_0)'$  and  $E_j = E'_j$ .
17:   end if
18: end for

```

To clarify this, we consider a simple case where the j -th eigenenergy is known to be in a range $E_j \in [E_j^L, E_j^U]$; moreover, we suppose other eigenenergies are far from this range. We expand the initial state in the eigenstate basis,

$$|\psi_0\rangle = \sum_{j=0}^{N-1} c_j |u_j\rangle. \quad (\text{B7})$$

We denote the square overlap of $|\psi\rangle$ and $|u_i\rangle$ to be

$$p_i = |\langle u_i | \psi \rangle|^2 = |c_i|^2. \quad (\text{B8})$$

For an energy value E in the range $[E_j^L, E_j^U]$, we calculate the ideal normalization factor $D_\tau(\psi_0)$,

$$\begin{aligned} D_\tau(\psi_0, E) &= \langle \psi | g^2(\tau(H - E)) | \psi \rangle \\ &= g^2(\tau(E_j - E))p_j + \sum_{i \neq j} g^2(\tau(E_i - E))p_i \\ &\approx g^2(\tau(E_j - E))p_j. \end{aligned} \quad (\text{B9})$$

The approximation holds when $g^2(\tau(E_j - E))p_j \gg g^2(\tau(E_i - E))p_i$. This naturally holds when the eigenenergies $\{E_i\}_{i \neq j}$ is far from the range $[E_j^L, E_j^U]$. From Eq. (B9) we can see that, the normalization factor takes the local maximum value close to p_j when the energy value $E = E_j$,

$$E_j = \underset{E \in [E_j^L, E_j^U]}{\text{argmax}} D_\tau(\psi_0, E). \quad (\text{B10})$$

Therefore, we can sweep the values of E in a range $[E_j^L, E_j^U]$ to search the largest value of $D_\tau(\psi_0, E)$. The eigenenergy searching algorithm is in Algorithm 2.

3. Unnormalized observable value estimation

Finally, we discuss the estimation $N_\tau(\psi_0, O)$ of a given observable $O = \sum_{l \in \mathcal{P}_n} o_l P_l$, where \mathcal{P}_n denotes the n -qubit Pauli group. o_l is the coefficient of the Pauli component P_l . We introduce the estimation algorithm of $N_\tau(\psi_0, O)$

Algorithm 3 Unnormalized eigenstate property estimation

Input: An n -qubit Hamiltonian H ; initial state $|\psi_0\rangle$ with nonzero overlap with j -th eigenstate of H : $p_j = |\langle u_j | \psi_0 \rangle|^2$; the energy E_j for the j -th eigenstate; the target observable $O = \sum_{l \in \mathcal{P}_n} o_l P_l$; cooling function $g(h)$ and the corresponding sampling probability $p(x)$; proper choice of the imaginary time τ , normalized cutoff time x_m .

Output: Estimation of the unnormalized observable value $N_\tau(\psi_0, O)$.

- 1: **for** $q = 1$ **to** N_M **do**
- 2: Sample two independent variables x_q and x'_q from $p(x)$.
- 3: **if** $x_q > x_m$ **or** $x'_q > x_m$ **then** ▷ Exceed the preset cutoff value
- 4: Set the estimation $\hat{n}_q = 0$.
- 5: **else** ▷ Normal single-shot quantum sampling by Hadamard test
- 6: Randomly sample a Pauli string $P(q)$ from the support of O , based on the probability distribution $\Pr(P(q) = P_l) = \frac{|o_l|}{\sum_{l \in \mathcal{P}_n} |o_l|}$. Denote $o(q) = o_l$.
- 7: Prepare an ancillary qubit on $|+\rangle$ state and the initial state $|\psi_0\rangle$.
- 8: Implement a controlled-unitary $C-V$ from the ancillary qubit to the state $|\psi_0\rangle$. Here, $V = e^{i\tau x_q^H} P(q) e^{i\tau x_q^H}$.
- 9: Generate a random bit b_q with a even distribution of values 0/1. Perform a gate S^{b_q} on the ancillary qubit.
- 10: Measure the ancillary qubit on X -basis, and record the binary result a_q . Then set the estimation value $\hat{n}_q = 2(-1)^{a_q} i^{b_q} e^{-i\tau(x_q - x'_q) E'_j}$.
- 11: **end if**
- 12: **end for**
- 13: Set the estimation of the unnormalized expectation value $\hat{N}_\tau^{x_m}(\psi_0, O) := \text{Re} \left(\frac{1}{N_M} \sum_{q=1}^{N_M} \frac{o(q)}{|o(q)|} \hat{n}_q \right)$.

Algorithm 4 Ground state property estimation

Input: An n -qubit Hamiltonian H ; initial state $|\psi_0\rangle$ with nonzero overlap with the ground state of H : $p_0 = |\langle u_0 | \psi_0 \rangle|^2$; the ground state energy E_0 ; the target observable $O = \sum_{l \in \mathcal{P}_n} o_l P_l$; cooling function $g(h)$ and the corresponding sampling probability $p(x)$; proper choice of the imaginary time τ , normalized cutoff time x_m .

Output: Estimation of the observable value $\langle u_0 | O | u_0 \rangle$ for the ground state.

- 1: Perform Algorithm 1 to output the estimation of the normalization factor $\hat{D}_\tau^{x_m}(\psi_0)$.
- 2: Perform Algorithm 3 to output the estimation of the unnormalized observable value $\hat{N}_\tau^{x_m}(\psi_0)$.
- 3: Output the estimation $\langle \hat{O} \rangle_{\psi(\tau)}^{x_m} = \frac{\hat{N}_\tau^{x_m}(\psi_0, O)}{\hat{D}_\tau^{x_m}(\psi_0)}$.

based on Eq. (B4) and the Hadamard test.

In the property estimation procedure, we sample a Pauli component P_l during each quantum experiment, and estimate its value. To enhance the sample efficiency, we introduce the $l1$ -importance sampling, that is, we sample different Pauli components based on the following probability distribution,

$$\Pr(P(q) = P_l) = \frac{|o_l|}{\sum_{l \in \mathcal{P}_n} |o_l|}. \quad (\text{B11})$$

The unnormalized eigenstate property estimation is shown in Algorithm 3.

To summarize, we list the algorithm for the two applications in the main text, shown in Algorithms 4 and 5.

Appendix C: Error and resource requirement analysis for quantum cooling algorithm

In this section, we study the estimation error caused by the finite quantum circuit depth and sampling number. Based on the error dependence, we estimate the resource requirements (i.e. circuit depth and sample number) of the cooling algorithm.

Here, we limit our analysis to the positive and even cooling function such that $g(h) = g(-h)$. Therefore,

$$g(\tau(H - E)) = g^\dagger(\tau(H - E)). \quad (\text{C1})$$

For simplicity, we first assume a precise eigenenergy estimation E_j of the j -th eigenstate. Later we discuss the effect of inaccurate E_j in the estimation procedure.

Algorithm 5 Eigenstate property estimation

Input: An n -qubit Hamiltonian H ; initial state $|\psi_0\rangle$ with nonzero overlap with the ground state of H : $p_0 = |\langle u_0|\psi_0\rangle|^2$; the energy interval $[E_j^L, E_j^U]$ for the j -th eigenstate; the target observable $O = \sum_{l \in \mathbb{P}_n} o_l P_l$; cooling function $g(h)$ and the corresponding sampling probability $p(x)$; proper choice of the imaginary time τ , normalized cutoff time x_m .

Output: Estimation of the observable value $\langle u_j|O|u_j\rangle$ for the j -th eigenstate.

- 1: Perform Algorithm 2 to output the estimation of the eigenenergy E_j and the normalization factor $\hat{D}_\tau^{x_m}(\psi_0)$.
- 2: Perform Algorithm 3 to output the estimation of the unnormalized observable value $\hat{N}_\tau^{x_m}(\psi_0)$.
- 3: Output the estimation $\langle \hat{O} \rangle_{\psi(\tau)}^{x_m} = \frac{\hat{N}_\tau^{x_m}(\psi_0, O)}{\hat{D}_\tau^{x_m}(\psi_0)}$.

In Fig. 4 we summarize our error analysis. In Sec. C 1, we consider the effect of finite imaginary time τ ; in Sec. C 2, we bound the estimation error caused by the normalized cutoff time x_m . The two factors above determine the actual maximum evolution time. In Sec. C 3, based on the measurement using Hadamard test, we determine the statistical error caused by finite sampling number N_M . Finally, we summarize the finite sampling effect in Sec. C 4 and show the dependence of circuit depth t_m and sampling number N_M with respect to the initial state $|\psi_0\rangle$, Hamiltonian H and the observable O .

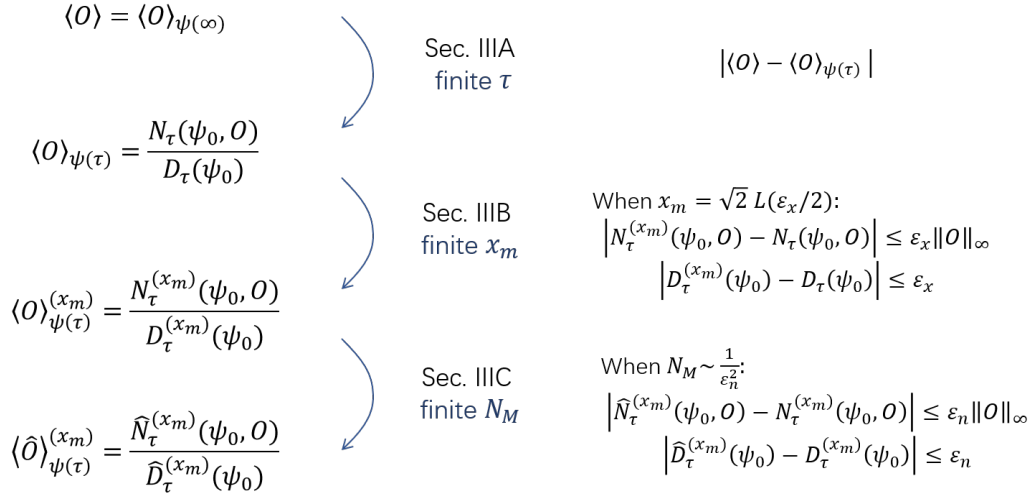


FIG. 4. Summary of the error analysis. Started from the ideal observation value $\langle O \rangle$, we sequentially study the effect of finite imaginary time τ , finite normalized cutoff time x_m and finite sampling number N_M .

1. Finite imaginary evolution time

To evaluate the effect of finite τ , we calculate the difference between $\langle O \rangle$ and $\langle O \rangle_{\psi(\tau)}$,

$$|\langle O \rangle_{\psi(\tau)} - \langle O \rangle| = \frac{|N_\tau(\psi_0, O) - D_\tau(\psi_0) \langle O \rangle|}{D_\tau(\psi_0)}. \quad (\text{C2})$$

Suppose we prepare a initial state $|\psi_0\rangle$ with a wavefunction

$$|\psi_0\rangle = \sum_{i=0}^{N-1} c_i |u_i\rangle. \quad (\text{C3})$$

We denote the amplitude $p_i := |c_i|^2$.

Perform a cooling operator $g(\tau(H - E_j))$ on the initial state $|\psi_0\rangle$, we have

$$g(\tau(H - E_j)) |\psi_0\rangle = c_j |u_j\rangle + \sum_{i \neq j} c_i g(\tau \Delta_{ij}) |u_i\rangle, \quad (\text{C4})$$

where $\Delta_{ij} := |E_i - E_j|$ is the energy difference between the i -th and j -th eigenstates.

Then the normalization factor $D_\tau(\psi_0)$ and the unnormalized observed value $N_\tau(\psi_0, O)$ are

$$\begin{aligned}
D_\tau(\psi_0) &= \langle \psi_0 | g^2(\tau(H - E_j)) | \psi_0 \rangle = p_j + \sum_{i \neq j} g^2(\tau\Delta_{ij}) p_i, \\
N_\tau(\psi_0, O) &= \left(c_j^* \langle u_j | + \sum_{k \neq j} c_k^* g(\tau\Delta_{kj}) \langle u_k | \right) O \left(c_j | u_j \rangle + \sum_{i \neq j} c_i g(\tau\Delta_{ij}) | u_i \rangle \right) \\
&= p_j \langle u_j | O | u_j \rangle + \sum_{i \neq j} [p_i g^2(\tau\Delta_{ij}) \langle u_i | O | u_i \rangle + g(\tau\Delta_{ij}) 2\text{Re}(c_i^* c_j \langle u_i | O | u_j \rangle)] \\
&\quad + \sum_{i, k \neq j} g(\tau\Delta_{ij}) g(\tau\Delta_{kj}) 2\text{Re}(c_i^* c_k \langle u_i | O | u_k \rangle).
\end{aligned} \tag{C5}$$

Therefore

$$\begin{aligned}
N_\tau(\psi_0, O) - D_\tau(\psi_0) \langle O \rangle &= \sum_{i \neq j} [p_i g^2(\tau\Delta_{ij}) (\langle u_i | O | u_i \rangle - \langle u_j | O | u_j \rangle) + g(\tau\Delta_{ij}) 2\text{Re}(c_i^* c_j \langle u_i | O | u_j \rangle)] \\
&\quad + \sum_{i, k \neq j} g(\tau\Delta_{ij}) g(\tau\Delta_{kj}) 2\text{Re}(c_i^* c_k \langle u_i | O | u_k \rangle) \\
&\approx \sum_{i \in \mathcal{N}(j)} g(\tau\Delta_{ij}) 2\text{Re}(c_i^* c_j \langle u_i | O | u_j \rangle),
\end{aligned} \tag{C6}$$

where $\mathcal{N}(j)$ is used to denote the index set of i where E_i is close to E_j such that the value of $g(\tau\Delta_{ij})$ is not ignorable. For example, for the triangular cooling function $\text{tri}(h)$, $\mathcal{N}(j)$ stands for the E_i such that $|E_i - E_j| \leq \frac{1}{\tau}$. Here, we assume τ is large, so that $g(\tau\Delta_{ij}) \ll p_j \langle u_j | O | u_j \rangle$ for $j \in \mathcal{N}(i)$. From Eq. (C6) we can approximately evaluate the difference between $\langle O \rangle$ and $\langle O \rangle_{\psi(\tau)}$,

$$\begin{aligned}
|\langle O \rangle_{\psi(\tau)} - \langle O \rangle| &= \frac{|N_\tau(\psi, O) - D_\tau(\psi_0) \langle O \rangle|}{D_\tau(\psi_0)} \\
&\approx \frac{\left| \sum_{i \in \mathcal{N}(j)} g(\tau\Delta_{ij}) 2\text{Re}(c_j^* c_i \langle u_j | O | u_i \rangle) \right|}{p_j} \\
&\leq \frac{2|c_j| \left\| O \right\|_\infty \sum_{i \in \mathcal{N}(j)} g(\tau\Delta_{ij}) |c_i|}{p_j},
\end{aligned} \tag{C7}$$

where $\|O\|_\infty$ is the maximum eigenvalue of the observable O . Eq. (C7) shows that, the requirement of imaginary evolution parameter τ is related to the energy interval Δ_{ij} , the form of the cooling function $g(h)$ and the overlap between the initial state and the j -th eigenstate p_j .

2. Finite normalized cutoff time

Now, we bound the estimation errors of $N_\tau(\psi_0, O)$ and $D_\tau(\psi_0)$ caused by the normalized cutoff time x_m . The estimation formula is given in Eq. (B4),

$$\begin{aligned}
D_\tau^{x_m}(\psi_0) &= \int_{-x_m}^{x_m} dy \tilde{p}(y) e^{-i\tau y E_j} \langle \psi_0 | e^{i\tau y H} | \psi_0 \rangle, \\
N_\tau^{x_m}(\psi_0, O) &= \int_{-x_m}^{x_m} dx \int_{-x_m}^{x_m} dx' p(x) p(x') \sum_{l \in \mathcal{P}_n} o_l e^{-i\tau(x-x') E_j} \langle \psi_0 | e^{-i\tau x' H} P_l e^{i\tau x' H} | \psi_0 \rangle.
\end{aligned} \tag{C8}$$

For the normalization factor $D_\tau^{x_m}(\psi_0)$ we have,

$$\begin{aligned}
|D_\tau^{x_m}(\psi_0) - D_\tau(\psi_0)| &\leq \left(\int_{x_m}^\infty + \int_{-\infty}^{-x_m} \right) dy |\tilde{p}(y) e^{-i\tau y E_j} \langle \psi_0 | e^{i\tau y H} | \psi_0 \rangle| \\
&\leq \left(\int_{x_m}^\infty + \int_{-\infty}^{-x_m} \right) dy \tilde{p}(y) =: \varepsilon_x^{(1)}.
\end{aligned} \tag{C9}$$

Recall that

$$\begin{aligned}\tilde{p}(y) &= \frac{1}{2} \int_{-\infty}^{\infty} p\left(\frac{z+y}{2}\right) p\left(\frac{z-y}{2}\right) dz \\ &= \int_{-\infty}^{\infty} p(t-y) p(t) dt = [p \star p](y).\end{aligned}\tag{C10}$$

We can show the following relationship between $\tilde{p}(y)$ and $p(x)$ by the nonnegativity of $p(x)$,

$$\begin{aligned}\int_{-x_m}^{x_m} \tilde{p}(y) dy &\geq \int_{-x_m/\sqrt{2}}^{x_m/\sqrt{2}} dx \int_{-x_m/\sqrt{2}}^{x_m/\sqrt{2}} dx' p(x) p(x') \\ &\geq (1 - L^{-1}\left(\frac{x_m}{\sqrt{2}}\right))^2 \\ &\geq 1 - 2L^{-1}\left(\frac{x_m}{\sqrt{2}}\right),\end{aligned}\tag{C11}$$

where $\varepsilon = L(x_m) = 1 - \int_{-x_m}^{x_m} p(x) dx$.

Therefore,

$$\begin{aligned}\varepsilon_x^{(1)} &= 1 - \int_{-x_m}^{x_m} \tilde{p}(y) dy \leq 2L^{-1}\left(\frac{x_m}{\sqrt{2}}\right), \\ \Rightarrow x_m &\leq \sqrt{2}L\left(\frac{\varepsilon_x^{(1)}}{2}\right).\end{aligned}\tag{C12}$$

For the unnormalized expectation value $N_{\tau}^{x_m}(\psi_0, O)$ we have,

$$\begin{aligned}|N_{\tau}^{x_m}(\psi_0, O) - N_{\tau}(\psi_0, O)| &\leq \iint_{\bar{S}} dx dx' p(x) p(x') \left| e^{-i\tau(x-x')E_j} \langle \psi_0 | e^{-i\tau x' H} O e^{i\tau x' H} | \psi_0 \rangle \right| \\ &\leq \iint_{\bar{S}} dx dx' p(x) p(x') \left| \langle \psi_0 | e^{-i\tau x' H} O e^{i\tau x' H} | \psi_0 \rangle \right| \\ &\leq \|O\|_{\infty} \iint_{\bar{S}} dx dx' p(x) p(x') =: \|O\|_{\infty} \varepsilon_x^{(2)},\end{aligned}\tag{C13}$$

where \bar{S} implies the complement area of $S : \{(x, x') | |x| \leq x_m, |x'| \leq x_m\}$.

We have

$$\begin{aligned}\varepsilon_x^{(2)} &= 1 - \iint_S dx dx' p(x) p(x') = 1 - (1 - L^{-1}(x_m))^2 \leq 2L^{-1}(x_m) \\ \Rightarrow x_m &\leq L\left(\frac{\varepsilon_x^{(2)}}{2}\right).\end{aligned}\tag{C14}$$

Therefore, when we choose the x_m to be $L(\varepsilon)$, we can achieve the estimation of $N_{\tau}(\psi_0, O)$ and $D_{\tau}(\psi_0)$ with a precession of $\|O\|_{\infty} \varepsilon$ and ε , respectively.

From Eq. (B4) we can see that, the maximum evolution time is $t_m = x_m \tau$. Combining the analysis in Sec. C1 and C2, we obtain the requirement of the quantum circuit depth.

3. Finite sample number

Now we consider the statistical fluctuation when estimating the values of $D_{\tau}^{x_m}(\psi_0)$ and $N_{\tau}^{x_m}(\psi_0, O)$ in Eq. (B4). In the single-shot version of Hadamard test in Algorithm 5, we can describe these identical and identically distributed (i.i.d.) single-round estimators for $D_{\tau}^{x_m}(\psi_0)$ and $N_{\tau}^{x_m}(\psi_0, O)$ as $\{\hat{d}_p\}_{p=1}^{N_M}$ and $\{\hat{n}_q\}_{q=1}^{N_M}$, respectively.

The single-round estimator \hat{d}_p is a random variable defined as follows,

$$\hat{d}_p = \begin{cases} \operatorname{Re}(2e^{-\tau y E_j}), & (b, a) = (0, 0), y : |y| \leq x_m \\ \operatorname{Re}(-2e^{-\tau y E_j}), & (b, a) = (0, 1), y : |y| \leq x_m \\ \operatorname{Re}(2ie^{-\tau y E_j}), & (b, a) = (1, 0), y : |y| \leq x_m \\ \operatorname{Re}(-2ie^{-\tau y E_j}), & (b, a) = (1, 1), y : |y| \leq x_m \\ 0, & y : |y| > x_m. \end{cases}\tag{C15}$$

Similarly, the single-round estimator \hat{n}_q is a random variable defined as follows,

$$\hat{n}_q = \begin{cases} \operatorname{Re}(2e^{-\tau(x-x')E_j}o(q)), & (b, a) = (0, 0), (x, x') : |x| \leq x_m, |x'| \leq x_m \\ \operatorname{Re}(-2e^{-\tau(x-x')E_j}o(q)), & (b, a) = (0, 1), (x, x') : |x| \leq x_m, |x'| \leq x_m \\ \operatorname{Re}(2ie^{-\tau(x-x')E_j}o(q)), & (b, a) = (1, 0), (x, x') : |x| \leq x_m, |x'| \leq x_m \\ \operatorname{Re}(-2ie^{-\tau(x-x')E_j}o(q)), & (b, a) = (1, 1), (x, x') : |x| \leq x_m, |x'| \leq x_m \\ 0, & (x, x') : |x| > x_m \text{ or } |x'| > x_m. \end{cases} \quad (\text{C16})$$

The final estimation of $D_\tau^{x_m}(\psi_0)$ and $N_\tau^{x_m}(\psi_0, O)$ is given by

$$\begin{aligned} \hat{D}_\tau^{x_m}(\psi_0) &= \frac{1}{N_M} \sum_{p=1}^{N_M} \hat{d}_p \\ \hat{N}_\tau^{x_m}(\psi_0, O) &= \frac{1}{N_M} \sum_{q=1}^{N_M} \hat{n}_q \end{aligned} \quad (\text{C17})$$

Based on Eq. (B4), we know that

$$\begin{aligned} \mathbb{E}_{(y, b, a)} \left(\hat{D}_\tau^{x_m}(\psi_0) \right) &= D_\tau^{x_m}(\psi_0), \\ \mathbb{E}_{(x, x', P, b, a)} \left(\hat{N}_\tau^{x_m}(\psi_0, O) \right) &= N_\tau^{x_m}(\psi_0, O). \end{aligned} \quad (\text{C18})$$

To analyze the statistical fluctuation, we apply the Hoeffding bound.

Lemma 1. (Hoeffding bound) For n independent random variables $\{\hat{X}_i\}_{i=1}^n$ which are bounded by $[a, b]$, the average value

$$\bar{X} := \frac{1}{n} \sum_{i=1}^n \hat{X}_i, \quad (\text{C19})$$

satisfies

$$\Pr(|\bar{X} - \mathbb{E}(\bar{X})| \geq \varepsilon) \leq 2 \exp \left(-\frac{2n\varepsilon^2}{(b-a)^2} \right). \quad (\text{C20})$$

Using Lemma 1, we conclude that

$$\begin{aligned} \Pr \left(|\hat{D}_\tau^{x_m}(\psi_0) - D_\tau^{x_m}(\psi_0)| \geq \varepsilon_n^{(1)} \right) &\leq 2 \exp \left(-\frac{2N_M(\varepsilon_n^{(1)})^2}{16} \right) =: \delta^{(1)}, \\ \Pr \left(|\hat{N}_\tau^{x_m}(\psi_0, O) - N_\tau^{x_m}(\psi_0, O)| \geq \varepsilon_n^{(2)} \|O\|_\infty^2 \right) &\leq 2 \exp \left(-\frac{2N_M(\varepsilon_n^{(2)})^2}{16} \right) =: \delta^{(2)}. \end{aligned} \quad (\text{C21})$$

Therefore, under the given precision $\varepsilon_n^{(1)}$ and $\varepsilon_n^{(2)}$, to keep the failure probability to a small value, the sampling number should satisfy $N_M \sim (\varepsilon_n^{(1)})^{-2}$ and $N_M \sim (\varepsilon_n^{(2)})^{-2}$.

4. Combined results

In Sec. C2 and Sec. C3, we estimate the errors caused by finite x_m and N_M , respectively. In summary, when we choose x_m to be $\max\{\sqrt{2}L(\frac{\varepsilon_x^{(1)}}{2}), L(\frac{\varepsilon_x^{(2)}}{2})\}$ and N_M to be $\max\{\alpha(\varepsilon_n^{(1)})^{-2}, \alpha(\varepsilon_n^{(2)})^{-2}\}$, then the following bound holds simultaneously

$$\begin{aligned} |\hat{D}_\tau^{x_m}(\psi_0) - D_\tau(\psi_0)| &\leq \varepsilon_n^{(1)} + \varepsilon_x^{(1)}, \\ |\hat{N}_\tau^{x_m}(\psi_0, O) - N_\tau(\psi_0, O)| &\leq (\varepsilon_n^{(2)} + \varepsilon_x^{(2)}) \|O\|_\infty, \end{aligned} \quad (\text{C22})$$

with a failure probability $\delta(\alpha) = 4e^{-\frac{\alpha}{8}}$.

Based on Eq. (C22), we bound the difference between the quotients $\langle \hat{O} \rangle_{\psi(\tau)}^{x_m}$ and $\langle O \rangle_\tau$,

$$\begin{aligned} \varepsilon_{x,n} := |\langle O \rangle_\tau - \langle \hat{O} \rangle_{\psi(\tau)}^{x_m}| &\leq \left| \frac{N_\tau(\psi_0, O)}{D_\tau(\psi_0)} - \frac{\hat{N}_\tau^{x_m}(\psi_0, O)}{\hat{D}_\tau^{x_m}(\psi_0)} \right| \\ &\leq \left| \frac{N_\tau(\psi_0, O)}{D_\tau(\psi_0)} - \frac{N_\tau(\psi_0, O) - (\varepsilon_n^{(2)} + \varepsilon_x^{(2)})\|O\|_\infty}{D_\tau(\psi_0) + (\varepsilon_n^{(1)} + \varepsilon_x^{(1)})} \right| \\ &\approx \frac{(\varepsilon_n^{(1)} + \varepsilon_x^{(1)})N_\tau(\psi_0, O) + (\varepsilon_n^{(2)} + \varepsilon_x^{(2)})\|O\|_\infty D_\tau(\psi_0)}{D_\tau^2(\psi_0)}. \end{aligned} \quad (\text{C23})$$

Combined with Eq. (C7), we have

$$\begin{aligned} |\langle \hat{O} \rangle_{\psi(\tau)}^{x_m} - \langle O \rangle| &\leq |\langle O \rangle_\tau - \langle \hat{O} \rangle_{\psi(\tau)}^{x_m}| + |\langle O \rangle_{\psi(\tau)} - \langle O \rangle| = \varepsilon_\tau + \varepsilon_{x,n} \\ &\approx \frac{(\varepsilon_n^{(1)} + \varepsilon_x^{(1)})N_\tau(\psi_0, O) + (\varepsilon_n^{(2)} + \varepsilon_x^{(2)})\|O\|_\infty D_\tau(\psi_0)}{D_\tau^2(\psi_0)} + \frac{2|c_j| \left| \|O\|_\infty \sum_{i \in \mathcal{N}(j)} g(\tau \Delta_{ij}) |c_i| \right|}{p_j}, \end{aligned} \quad (\text{C24})$$

Recall from Eq. (C5) that

$$\begin{aligned} D_\tau(\psi_0) &= \langle \psi_0 | g^2(\tau(H - E_j)) | \psi_0 \rangle = p_j + \sum_{i \neq j} g^2(\tau \Delta_{ij}) p_i \approx p_j, \\ N_\tau(\psi_0, O) &= p_j \langle u_j | O | u_j \rangle + \sum_{i \neq j} [p_i g^2(\tau \Delta_{ij}) \langle u_i | O | u_i \rangle + g(\tau \Delta_{ij}) 2\text{Re}(c_i^* c_j \langle u_i | O | u_j \rangle)] \\ &\quad + \sum_{i, k \neq j} g(\tau \Delta_{ij}) g(\tau \Delta_{kj}) 2\text{Re}(c_i^* c_k \langle u_i | O | u_k \rangle) \approx p_j \langle O \rangle, \end{aligned} \quad (\text{C25})$$

we then simplify Eq. (C24),

$$|\langle \hat{O} \rangle_{\psi(\tau)}^{x_m} - \langle O \rangle| \approx \frac{(\varepsilon_n^{(1)} + \varepsilon_x^{(1)}) \langle O \rangle + (\varepsilon_n^{(2)} + \varepsilon_x^{(2)})\|O\|_\infty}{p_j} + \frac{2|c_j| \left| \|O\|_\infty \sum_{i \in \mathcal{N}(j)} g(\tau \Delta_{ij}) |c_i| \right|}{p_j}. \quad (\text{C26})$$

To summarize, we have the following proposition,

Proposition 1. *In the eigenstate property estimation task in Algorithm 5, when we choose x_m to be $\max\{\sqrt{2}L(\frac{\varepsilon_x^{(1)}}{2}), L(\frac{\varepsilon_x^{(2)}}{2})\}$ and N_M to be $\max\{\alpha(\varepsilon_n^{(1)})^{-2}, \alpha(\varepsilon_n^{(2)})^{-2}\}$, then the estimated observable value satisfy*

$$\varepsilon := |\langle \hat{O} \rangle_{\psi(\tau)}^{x_m} - \langle O \rangle| \approx \frac{(\varepsilon_n^{(1)} + \varepsilon_x^{(1)}) \langle O \rangle + (\varepsilon_n^{(2)} + \varepsilon_x^{(2)})\|O\|_\infty}{p_j} + \frac{2|c_j| \left| \|O\|_\infty \sum_{i \in \mathcal{N}(j)} g(\tau \Delta_{ij}) |c_i| \right|}{p_j}, \quad (\text{C27})$$

with a failure probability $\delta(\alpha) = 4e^{-\frac{\alpha}{2}}$.

To simplify the discussion, we assume $\varepsilon_x := \varepsilon_x^{(1)} = \varepsilon_x^{(2)}$ and $\varepsilon_n := \varepsilon_n^{(1)} = \varepsilon_n^{(2)}$. Recall that

$$\begin{aligned} \varepsilon_\tau &\approx \frac{2|c_j| \left| \|O\|_\infty \sum_{i \in \mathcal{N}(j)} g(\tau \Delta_{ij}) |c_i| \right|}{p_j} \\ \varepsilon_{x,n} &\approx \frac{(\varepsilon_n^{(1)} + \varepsilon_x^{(1)})(\langle O \rangle + \|O\|_\infty)}{p_j} \end{aligned} \quad (\text{C28})$$

If we denote the total error by ε , we can choose $\varepsilon_\tau \sim \varepsilon_{x,n} \sim \varepsilon$ and further $\varepsilon_n \sim \varepsilon_x \sim \varepsilon p_j (\langle O \rangle + \|O\|_\infty)^{-1}$. This implies,

$$\begin{aligned} x_m &\sim L\left(\frac{\varepsilon p_j}{\langle O \rangle + \|O\|_\infty}\right) = \mathcal{O}\left(\text{poly}\left(\frac{\langle O \rangle + \|O\|_\infty}{\varepsilon p_j}\right)\right), \\ N_M &\sim \mathcal{O}\left(\frac{(\langle O \rangle + \|O\|_\infty)^2}{(\varepsilon p_j)^2}\right). \end{aligned} \quad (\text{C29})$$

We remark that, when the cooling function $g(h)$ is Gaussian or hyperbolic secant function, the dependence of x_m with p_j can be improved to

$$x_m \sim L\left(\frac{\varepsilon p_j}{\langle O \rangle + \|O\|_\infty}\right) = \mathcal{O}\left(\log\left(\frac{\langle O \rangle + \|O\|_\infty}{\varepsilon p_j}\right)\right). \quad (\text{C30})$$

For the finite τ error ε_τ , we further simplify the discuss by assume that the initial state only have nonzero overlap with the target eigenstate $|u_j\rangle$ and a neighbour eigenstate $|u_{j+1}\rangle$. We have,

$$\varepsilon \sim \frac{g(\tau \Delta_{j,j+1}) |c_{j+1}| |c_j|}{p_j}. \quad (\text{C31})$$

Therefore, the requirement of τ is

$$\tau \sim \mathcal{O}\left(\frac{1}{\Delta_{j,j+1}} g^{-1}(\varepsilon p_j)\right), \quad (\text{C32})$$

where $g^{-1}(p)$ is the inverse function of $g(h)$ when $h > 0$. g^{-1} characterize the requirement of τ given the target cooling value p . As is shown in Eqs. (A17), (A37), (A46), and (A55), the common cooling functions satisfy

$$g^{-1}(p) = \mathcal{O}\left(\log\left(\frac{1}{p}\right)\right), \quad (\text{C33})$$

that is, with a logarithm increasing τ , we can suppress the error term caused by finite imaginary time evolution.

To summarize, the circuit complexity of Algorithm 5 is

$$t_m = \tau x_m \sim \max_i \{\Delta_{ij}^{-1}\} L\left(\frac{\varepsilon p_j}{\langle O \rangle + \|O\|_\infty}\right) g^{-1}(\varepsilon p_j) = \max_i \{\Delta_{ij}^{-1}\} \mathcal{O}\left(\text{poly}\left(\frac{\langle O \rangle + \|O\|_\infty}{\varepsilon p_j}\right)\right), \quad (\text{C34})$$

and the sample complexity is

$$N_M \sim \mathcal{O}\left(\frac{(\langle O \rangle + \|O\|_\infty)^2}{(\varepsilon p_j)^2}\right). \quad (\text{C35})$$